Supporting Information

Mechanistic insights of anionic ligand exchange and fullerene reduction with magnesium(I) compounds

Samuel R. Lawrence, David B. Cordes, Alexandra M. Z. Slawin, Andreas Stasch*

EaStCHEM School of Chemistry, University of St Andrews, North Haugh, St Andrews, KY16 9ST, United Kingdom. E-mail: as411@st-andrews.ac.uk.

Table of Contents

1 Experimental Section

1.1 General considerations

All manipulations were carried out using standard Schlenk and glove box techniques under an atmosphere of high purity argon or dinitrogen. Benzene, toluene, *n*-hexane, *n*-pentane and THF were either dried and distilled under inert gas over $LiAlH_4$, sodium or potassium, or taken from an MBraun solvent purification system and degassed prior to use. ^{1}H, $^{13}C\{^{1}H\}$, and $^{31}P\{^{1}H\}$ NMR spectra were recorded on a Bruker AV 300, Bruker AVII 400 or Bruker AV III 500 spectrometer in deuterated benzene, toluene or THF and were referenced to the residual ^{1}H or $^{13}C\{^{1}H\}$ resonances of the solvent used, or external aqueous H_3PO_4 solutions, respectively. Selected NMR spectra are collected in section 2. IR spectra were recorded on neat solids using a Perkin Elmer Spectrum GX IR (ATR) spectrometer. Melting points were determined in sealed glass capillaries under argon and are uncorrected. Elemental analyses were performed by the Elemental Analysis Service at London Metropolitan University. C_{60} was purchased from Alfa Aesar (99 %) and stored in a glove box. The syntheses of $[\{(^{Ar}nacnac)Mg\}_2]$ **1** (**1a** Ar = Dip,[1] **1b** Ar = Dep,[2] **1c** Ar = Mes,[3] **1d** Ar = Xyl[4])[5], $[(\{Ph_2P(NDip)_2\}Mg)_2]$ **2**[6], and $[\{Ph_2P(NDip)_2\}Li]$ **6**[7] were performed according to literature procedures. Syntheses of $[\{(^{Ar}nacnac)Mg\}_nC_{60}]$ complexes,[8] $[(^{Dip}nacnac)MgMg(^{Mes}nacnac)]$ **4ac**,[9] $[(^{Mes}nacnac)Li]$ **5c**[10] and $[(^{Xyl}nacnac)Li]$ **5d**[8] have been reported previously. All other reagents were used as received from commercial sources. Abbreviations: s = singlet, d = doublet, t = triplet, q = quartet, sept = septet, br = broad, vbr = very broad, m = multiplet.

Attempts to isolate asymmetrically substituted magnesium(I) dimers (**4**, **7**) as pure samples in crystalline form from small scale reactions have failed so far and often, a symmetrically substituted complex, *e.g.* **1c**, was obtained.

1.2 Anionic ligand exchange reactions involving [{(^{Ar}nacnac)Mg}$_2$] 1 and [(^{Ar}nacnac)Li] 5 species

1.2.1 Reactions of [{(^{Ar}nacnac)Mg}$_2$] 1 with [{($^{Ar'}$nacnac)Mg}$_2$] 1'

[(^{Dip}nacnac)MgMg(^{Dep}nacnac)] 4ab

[{(^{Dip}nacnac)Mg}$_2$] **1a** (11.4 mg, 12.9 µmol) and [{(^{Dep}nacnac)Mg}$_2$] **1b** (10.0 mg, 13.0 µmol) were added to an NMR tube with J. Young valve and dissolved in benzene-d_6 (0.6 mL). The tube was charged with a catalytic amount of C_{60} (1.0 mg, 1.4 µmol, 10.7 mol%) and the reaction was followed using ^{1}H NMR spectroscopy at intervals. A stable equilibrium for the optimum formation of [(^{Dip}nacnac)MgMg(^{Dep}nacnac)] **4ab** was established after leaving the sample for seven days at 70°C (approx. ^{1}H NMR yield: 30%). (N.B. Prolonged heating led to the gradual decomposition of [{($^{Ar/Ar'}$nacnac)Mg}$_2$] to "homoleptic" magnesium(II) complexes [($^{Ar/Ar'}$nacnac)$_2$Mg].) Separation of products was not possible so far. ^{1}H NMR (499.9 MHz, benzene-d_6, 294 K) δ = 0.97 (d, J = 6.9 Hz, 12H; CH(CH_3)$_2$), 1.10 (t, J = 7.6 Hz, 12H; CH$_2$CH_3), 1.12 (d, J = 6.9 Hz, 12H; CH(CH_3)$_2$), 1.46 (s, 6H; NCCH_3), 1.60 (s, 6H; NCCH_3), 2.24 (dq, J = 15.2, 7.6 Hz, 4H; CH_2CH$_3$), 2.41 (dq, J = 15.2, 7.6 Hz, 4H; CH_2CH$_3$), 3.01 (sept, J = 6.9 Hz, 4H; CH(CH$_3$)$_2$), 4.82 (s, 1H; γ-CH), 4.87 (s, 1H; γ-CH), 6.88-7.15 (m, 12H; Ar-H).

[(^{Dip}nacnac)MgMg(^{Mes}nacnac)] 4ac

[{(^{Dip}nacnac)Mg}$_2$] **1a** (12.0 mg, 13.6 µmol) and [{(^{Mes}nacnac)Mg}$_2$] **1c** (10.0 mg, 14.0 µmol) were added to an NMR tube with J. Young valve, dissolved in benzene-d_6 (0.6 mL) and left standing at room temperature. The solution was left standing at room temperature and the reaction followed by ^{1}H NMR spectroscopy at regular intervals. A very slow scrambling reaction was observed; an equilibrium was reached approximately after two months (59 days) (**1a**:**1c**:**4ac** ratio of 5:1:8) accompanied by considerable decomposition to [(^{Mes}nacnac)$_2$Mg] (*ca*. 25% of all species present in solution). Repeating the reaction using an additional catalytic quantity of C_{60} (1.0 mg, 1.39 µmol, 10 mol%) allowed the reaction to proceed at a similar rate, giving a comparable concentration of products after 60 days at room temperature (**1a**:**1c**:**4ac** ratio of 2:1:4), but with significantly less decomposition product [(^{Mes}nacnac)$_2$Mg] (*ca.* 4% of all species present in solution). ^{1}H NMR (499.9 MHz, benzene-d_6, 295 K) δ = 1.01 (d, J = 6.9 Hz, 12H), 1.13 (d, J = 6.9 Hz, 12H), 1.47 (s, 6H), 1.65 (s, 6H), 1.90 (s, 12H), 2.30 (s, 6H), 3.02 (sept, J = 6.9 Hz, 4H), 4.83 (s, 1H), 4.88 (s, 1H), 6.77 (s, 4H), 6.95-7.15 (m, 6H). ^{1}H NMR spectroscopic data are identical to those reported in the literature.[9]

[($^{\text{Dep}}$nacnac)MgMg($^{\text{Mes}}$nacnac)] 4bc

[{($^{\text{Dep}}$nacnac)Mg}$_2$] **1b** (26.2 mg, 34.0 μmol) and [{($^{\text{Mes}}$nacnac)Mg}$_2$] **1c** (24.3 mg, 34.0 μmol) were added to an NMR tube with J. Young valve, dissolved in benzene-*d*$_6$ (0.6 mL), and left standing at room temperature. An equilibrium of products was established after *ca.* 22 h, as observed by ^{1}H NMR spectroscopy (**1b**:**1c**:**4bc** ratio of 1:1:2). ^{1}H NMR (499.9 MHz, benzene-*d*$_6$, 294 K) δ = 1.07 (t, J = 8.3 Hz, 12H; CH_2CH$_3$), 1.53 (s, 6H; $^{\text{Dep}}$NCCH_3), 1.57 (s, 6H; $^{\text{Mes}}$NCCH_3), 1.90 (s, 12H; *o*-CH_3), 2.29 (s, 6H; *p*-CH_3), 2.30 (dq, J = 15.2, 7.7 Hz, 4H; CH_2CH$_3$), 2.33 (dq, J = 15.2, 7.7 Hz, 4H; CH_2CH$_3$), 4.80 (s, 1H; $^{\text{Mes}}\gamma$-C*H*), 4.81 (s, 1H; $^{\text{Dep}}\gamma$-C*H*), 6.83 (s, 4H; $^{\text{Mes}}$Ar-*H*), 7.05-7.13 (m, 6H; $^{\text{Dep}}$Ar-*H*). ^{13}C{^{1}H} NMR (125.7 MHz, benzene-*d*$_6$, 295 K) δ = 14.6 ($^{\text{Dep}}$NC*C*H$_3$), 19.3 ($^{\text{Mes}}$NC*C*H$_3$), 21.1 ($^{\text{Mes}}$*p*-*C*H$_3$), 23.2 ($^{\text{Mes}}$*o*-*C*H$_3$), 23.5 ($^{\text{Dep}}$CH$_2$*C*H$_3$), 25.3 ($^{\text{Dep}}$*C*H$_2$CH$_3$), 95.2 ($^{\text{Mes}}$CH), 95.6 ($^{\text{Dep}}$*C*H), 124.6 ($^{\text{Dep}}$Ar-*C*), 126.1 ($^{\text{Dep}}$Ar-*C*), 129.2 ($^{\text{Mes}}$Ar-*C*), 132.7 ($^{\text{Mes}}$Ar-*C*), 137.3 ($^{\text{Dep}}$Ar-*C*), 145.6 ($^{\text{Mes}}$Ar-*C*), 146.7 ($^{\text{Dep}}$Ar-*C*), 166.6 ($^{\text{Mes}}$N*C*CH$_3$), 166.7 ($^{\text{Dep}}$N*C*CH$_3$).

[($^{\text{Dep}}$nacnac)MgMg($^{\text{Xyl}}$nacnac)] 4bd

[{($^{\text{Dep}}$nacnac)Mg}$_2$] **1b** (9.7 mg, 12.6 μmol) and [{($^{\text{Xyl}}$nacnac)Mg}$_2$] **1d** (8.4 mg, 12.7 μmol) were added to an NMR tube with J. Young valve, dissolved in benzene-*d*$_6$ (0.6 mL) and left standing at room temperature. An equilibrium of products was established after *ca.* 19 h, as observed by ^{1}H NMR spectroscopy (**1b**:**1d**:**4bd** ratio of 1:1:2). ^{1}H NMR (499.9 MHz, benzene-*d*$_6$, 295 K) δ = 1.07 (t, J = 7.6 Hz, 12H; CH_2CH$_3$), 1.47 (s, 6H; NCCH_3), 1.57 (s, 6H; NCCH_3), 1.91 (s, 12H; $^{\text{Xyl}}$*o*-CH_3), 2.31 (two overlapping dq, J = 15.5, 7.7 Hz, 8H; CH$_2$CH_3), 4.77 (s, 1H; $^{\text{Xyl}}\gamma$-C*H*), 4.81 (s, 1H; $^{\text{Dep}}\gamma$-C*H*), 6.91-7.14 (m, 12H; Ar-*H*); ^{13}C{^{1}H} NMR (125.7 MHz, benzene-*d*$_6$, 295 K) δ = 14.7 ($^{\text{Dep}}$NC*C*H$_3$), 19.4 ($^{\text{Xyl}}$NC*C*H$_3$), 23.2 ($^{\text{Xyl}}$*o*-*C*H$_3$), 23.5 ($^{\text{Dep}}$CH$_2$*C*H$_3$), 25.3 ($^{\text{Dep}}$*C*H$_2$CH$_3$), 95.2 ($^{\text{Xyl}}$*C*H), 95.5 ($^{\text{Dep}}$*C*H), 124.1 ($^{\text{Xyl}}$Ar-*C*), 124.6 ($^{\text{Dep}}$Ar-*C*), 126.5 ($^{\text{Dep}}$Ar-*C*), 128.5 ($^{\text{Xyl}}$Ar-*C*), 131.8 ($^{\text{Xyl}}$Ar-*C*), 137.3 ($^{\text{Dep}}$Ar-*C*), 146.7 ($^{\text{Dep}}$Ar-*C*), 148.3 ($^{\text{Xyl}}$Ar-*C*), 166.4 ($^{\text{Xyl}}$N*C*CH$_3$), 166.8 ($^{\text{Dep}}$N*C*CH$_3$).

[($^{\text{Mes}}$nacnac)MgMg($^{\text{Xyl}}$nacnac)] 4cd

[{($^{\text{Mes}}$nacnac)Mg}$_2$] **1c** (8.0 mg, 11.2 μmol) and [{($^{\text{Xyl}}$nacnac)Mg}$_2$] **1d** (7.4 mg, 11.2 μmol) were added to an NMR tube with J. Young valve and dissolved in benzene-*d*$_6$ (0.6 mL). Within five minutes an equilibrium of products was established, as observed by ^{1}H NMR spectroscopy (**1c**:**1d**:**4cd** ratio of 1:1:2). ^{1}H NMR (499.9 MHz, benzene-*d*$_6$, 295 K) δ = 1.50 (s, 6H; $^{\text{Xyl}}$NCCH_3), 1.55 (s, 6H; $^{\text{Mes}}$NCCH_3), 1.91 (br. s, 24H; $^{\text{Xyl}}$*o*-CH_3 + $^{\text{Mes}}$*o*-CH_3), 2.28 (s, 6H; $^{\text{Mes}}$*p*-CH_3), 4.77 (s, 1H; $^{\text{Xyl}}\gamma$-C*H*), 4.80 (s, 1H; $^{\text{Mes}}\gamma$-C*H*), 6.84 (s, 4H; $^{\text{Mes}}$Ar-*H*), 6.92-7.06 (m, 6H; $^{\text{Xyl}}$Ar-*H*); ^{13}C{^{1}H} NMR (125.7 MHz, benzene-*d*$_6$, 295 K) δ = 19.26 ($^{\text{Mes}}$NC*C*H$_3$), 19.28 ($^{\text{Xyl}}$NC*C*H$_3$), 21.11 ($^{\text{Mes}}$*p*-*C*H$_3$), 23.15 ($^{\text{Xyl}}$*o*-*C*H$_3$), 23.18 ($^{\text{Mes}}$*o*-*C*H$_3$), 95.4 (*C*H), 124.2 ($^{\text{Xyl}}$Ar-*C*), 128.45 ($^{\text{Xyl}}$Ar-*C*), 129.22

(^{Mes}Ar-*C*), 131.4 (^{Mes}Ar-*C*), 131.8 (^{Xyl}Ar-*C*), 132.7 (^{Mes}Ar-*C*), 145.4 (^{Mes}Ar-*C*), 148.1 (^{Xyl}Ar-*C*), 166.3 (^{Xyl}N*C*CH$_3$), 166.6 (^{Mes}N*C*CH$_3$).

[{(^{Mes}nacnac)Mg}$_2$] **1c** (5.0 mg, 6.99 μmol) and [{(^{Xyl}nacnac)Mg}$_2$] **1d** (4.6 mg, 6.99 μmol) were added to an NMR tube with J. Young valve and dissolved in deuterated cyclohexane (0.6 mL). Within five minutes an equilibrium of products was established, as observed by ^{1}H NMR spectroscopy (**1c**:**1d**:**4cd** ratio of 1:1:2). ^{1}H NMR (499.9 MHz, cyclohexane-*d*$_{12}$, 295 K) δ = 1.43/1.44 (2 overlapping s, 6H; ^{Xyl}NCC*H*$_3$; 6H; ^{Mes}NCC*H*$_3$), 1.72 (s, 12H; ^{Mes}*o*-C*H*$_3$), 1.77 (s, 12H; ^{Xyl}*o*-C*H*$_3$), 2.27/2.28 (2 overlapping s, 6H; ^{Mes}*p*-C*H*$_3$), 4.60 (s, 1H; ^{Mes}γ-C*H*), 4.63 (s, 1H; ^{Xyl}γ-C*H*), 6.72 (s, 4H; ^{Mes}Ar-*H*), 6.82-6.86 (m, 6H; ^{Xyl}Ar-*H*).

[(^{Mes}nacnac)Mg(THF)Mg(THF)(^{Xyl}nacnac)] 4cd-THF

[{(^{Mes}nacnac)Mg}$_2$] **1c** (8.0 mg, 11.18 μmol) and [{(^{Xyl}nacnac)Mg}$_2$] **1d** (7.4 mg, 11.22 μmol) were added to an NMR tube with J. Young valve and dissolved in THF-*d*$_8$ (0.6 mL), giving an orange-red solution of **1c-THF** and **1d-THF**. No scrambling reactivity was observed after leaving for seven days at room temperature as judged by ^{1}H NMR spectroscopy. Heating at 50°C was required for a significant proportion of an exchange product to form and the reaction only proceeded very slowly. For example, a ratio of **1c-THF**:**1d-THF**:**4cd-THF** 1:1:1.5 was reached after leaving the solution at this temperature for approximately 29 days. ^{1}H NMR (499.9 MHz, THF-*d*$_8$, 295 K) δ = 1.38 (s, 6H; ^{Xyl}NCC*H*$_3$), 1.38 (s, 6H; ^{Mes}NCC*H*$_3$), 1.74 (s, 12H; ^{Mes}*o*-C*H*$_3$), 1.80 (s, 12H; ^{Xyl}*o*-C*H*$_3$), 2.24 (s, 6H; ^{Mes}*p*-C*H*$_3$), 4.53 (s, 1H; ^{Mes}γ-C*H*), 4.56 (s, 1H; ^{Xyl}γ-C*H*), 6.73 (s, 4H; ^{Mes}Ar-*H*), 6.79 (t, J_{HH} = 7.4 Hz, 2H; ^{Xyl}*p*-Ar-*H*), 6.92 (d, J_{HH} = 7.4 Hz, 4H; ^{Xyl}*m*-Ar-*H*). Note: some assignment of resonances to Mes versus Xyl substituents is tentative only.

1.2.2 [(^{Ar}nacnac)Li] 5

[(^{Mes}nacnac)Li] 5c

A hexane solution of *n*-butyllithium (1.6 M, 5.96 mL, 9.53 mmol, 1.10 equiv.) was slowly added to a cooled (0°C) solution of ^{Mes}nacnacH (2.90 g, 8.67 mmol) in *n*-hexane (30 mL) and stirred for 16 h at room temperature. Storing the reaction mixture at -40°C for one day afforded a white powder of **5c** which was filtered off and dried under vacuum. Concentrating the filtrate to *ca.* 10 mL and storing at -40°C for a further day afforded a second crop of **5c**. Yield = 2.60 g (88 %); ^{1}H NMR (499.9 MHz, benzene-*d*$_6$, 295 K) δ = 1.70 (s, 6H; NCC*H*$_3$), 2.04 (s, 12H; *o*-C*H*$_3$), 2.32 (s, 6H; *p*-C*H*$_3$), 4.80 (s, 1H; γ-C*H*), 6.94 (s, 4H; Ar-*H*); ^{1}H NMR spectroscopic data are identical to those reported in the literature.[9] M.p.: yellow colouration at *ca.* 135°C, some decomposition 182-184°C, full melting at 192-196°C.

1.2.3 Reaction of $[\{(^{Ar'}\mathrm{nacnac})\mathrm{Mg}\}_2]$ 1 with $[(^{Ar}\mathrm{nacnac})\mathrm{Li}]$ 5

Method 1: $[\{(^{Xyl}\mathrm{nacnac})\mathrm{Mg}\}_2]$ **1d** (7.4 mg, 11.2 μmol) and $[(^{Mes}\mathrm{nacnac})\mathrm{Li}]$ (7.6 mg, 22.3 μmol, 1.99 equiv.) **5c** were added to an NMR tube with J. Young valve, dissolved in benzene-d_6 (0.6 mL) and left standing at room temperature. No significant ligand exchange was observed by ^{1}H NMR spectroscopy at room temperature. Heating the sample to 50°C for six days gave a mixture of products in varying concentrations: $[\{(^{Mes}\mathrm{nacnac})\mathrm{Mg}\}_2]$ **1c**, $[\{(^{Xyl}\mathrm{nacnac})\mathrm{Mg}\}_2]$ **1d**,$[(^{Mes}\mathrm{nacnac})\mathrm{Li}]$ **5c**, $[(^{Xyl}\mathrm{nacnac})\mathrm{Li}]$ **5d**, and $[(^{Mes}\mathrm{nacnac})\mathrm{MgMg}(^{Xyl}\mathrm{nacnac})]$ **4cd**. Over time a magnesium mirror was deposited onto the inside of the NMR tube from thermal decomposition of $[\{(^{Ar}\mathrm{nacnac})\mathrm{Mg}\}_2]$ complexes and supported by concomitant formation $[\{(^{Ar}\mathrm{nacnac})_2\mathrm{Mg}\}]$ complexes.

Method 2: $[\{(^{Mes}\mathrm{nacnac})\mathrm{Mg}\}_2]$ **1c** (8.0 mg, 11.2 μmol) and $[(^{Xyl}\mathrm{nacnac})\mathrm{Li}]$ **5d** (7.0 mg, 22.3 μmol, 2.00 equiv.) were added to an NMR tube with J. Young valve, dissolved in benzene-d_6 (0.6 mL) and left standing at room temperature. No significant ligand exchange was observed by ^{1}H NMR spectroscopy at room temperature. Heating the sample to 50°C for six days gave a mixture of products in varying concentrations: $[\{(^{Mes}\mathrm{nacnac})\mathrm{Mg}\}_2]$ **1c**, $[\{(^{Xyl}\mathrm{nacnac})\mathrm{Mg}\}_2]$ **1d**, $[(^{Mes}\mathrm{nacnac})\mathrm{Li}]$ **5c**, $[(^{Xyl}\mathrm{nacnac})\mathrm{Li}]$ **5d**, and $[(^{Mes}\mathrm{nacnac})\mathrm{MgMg}(^{Xyl}\mathrm{nacnac})]$ **4cd**. Over time a magnesium mirror was deposited onto the inside of the NMR tube from thermal decomposition of $[\{(^{Ar}\mathrm{nacnac})\mathrm{Mg}\}_2]$ complexes and supported by concomitant formation $[\{(^{Ar}\mathrm{nacnac})_2\mathrm{Mg}\}]$ complexes.

1.3 Anionic ligand exchange reactions involving complexes with $(^{Ar}\mathrm{Nacnac})$ and $\{\mathrm{Ph_2P(NDip)_2}\}$ ligands

1.3.1 Reaction of $[\{(^{Mes}\mathrm{nacnac})\mathrm{Mg}\}_2]$ 1c with $[(\{\mathrm{Ph_2P(NDip)_2}\}\mathrm{Mg})_2]$ 2

$[\{(^{Mes}\mathrm{nacnac})\mathrm{Mg}\}_2]$ **1c** (9.0 mg, 12.6 μmol) and $[(\{\mathrm{Ph_2P(NDip)_2}\}\mathrm{Mg})_2]$ **2** (14.1 mg, 12.6 μmol, 1.00 equiv.) were added to an NMR tube with J. Young valve, benzene-d_6 (0.6 mL) was added, and the mixture was stored at room temperature. After ten days, a near equilibrium mixture had formed containing both starting materials, **1c** and **2**, and the mixed dimagnesium(I) species $[\{\mathrm{Ph_2P(NDip)_2}\}\mathrm{MgMg}(^{Mes}\mathrm{nacnac})]$ **7c** in an approximate 1:1:2 ratio, respectively. A small amount of decomposition product $[(^{Mes}\mathrm{nacnac})_2\mathrm{Mg}]$ was present (*ca.* 12%).

NMR data for **$[\{\mathrm{Ph_2P(NDip)_2}\}\mathrm{MgMg}(^{Mes}\mathrm{nacnac})]$ 7c**: ^{1}H NMR (499.9 MHz, benzene-d_6, 295 K,) δ = 0.96 (d, J_{HH} = 6.4 Hz, 24H; $^{NPN}\mathrm{CH(C}H_3)_2$), 1.61 (s, 6H; $^{Mes}\mathrm{NCC}H_3$), 2.08 (s, 12H; $^{Mes}o\text{-C}H_3$), 2.26 (s, 6H; $^{Mes}p\text{-C}H_3$), 3.60 (sept, J_{HH} = 6.8 Hz, 4H; $^{NPN}\mathrm{C}H(\mathrm{CH_3})_2$), 4.88 (s, 1H; $^{Mes}\gamma\text{-C}H$), 6.74-6.93 (m, 8H; $^{NPN}\mathrm{Ar}\text{-}H$), 6.80 (s, 4H; $^{Mes}\mathrm{Ar}\text{-}H$), 7.04-7.12 (m, 4H; $^{NPN}\mathrm{Ar}\text{-}H$), 7.14-7.21 (m, 4H; $^{NPN}\mathrm{Ph}\text{-}H$); ^{31}P NMR (202.4 MHz, benzene-d_6, 295 K) δ = 5.75.

1.3.2 Reaction of [{(^{Mes}nacnac)Mg}$_2$] 1c with [{Ph$_2$P(NDip)$_2$}Li] 6: formation of [{Ph$_2$P(NDip)$_2$}MgMg(^{Mes}nacnac)] 7c

[{(^{Mes}nacnac)Mg}$_2$] **1c** (6.4 mg, 8.9 µmol) and [{Ph$_2$P(NDip)$_2$}Li] **6** (9.7 mg, 17.9 µmol, 2.00 equiv.) were added to an NMR tube with J. Young valve, benzene-d_6 (0.6 mL) was added, and the mixture was heated to 50°C. After three and a half days at this temperature a mixture of products in varying concentrations had formed: [{(^{Mes}nacnac)Mg}$_2$] **1c**, [(^{Mes}nacnac)Li] **5c**, [{Ph$_2$P(NDip)$_2$}Li] **6**, [{Ph$_2$P(NDip)$_2$}MgMg(^{Mes}nacnac)] **7c** and [({Ph$_2$P(NDip)$_2$}Mg)$_2$] **2**. Over time a magnesium mirror deposited onto the inside of the NMR tube from partial thermal decomposition of [LMgMgL'] to [LMgL'] complexes.

1.3.2 Reaction of [({Ph$_2$P(NDip)$_2$}Mg)$_2$] 2 with [(^{Mes}nacnac)Li] 5c: formation of [{Ph$_2$P(NDip)$_2$}MgMg(^{Mes}nacnac)] 7c

[({Ph$_2$P(NDip)$_2$}Mg)$_2$] **2** (10.0 mg, 8.93 µmol) and [(^{Mes}nacnac)Li] **5c** (6.1 mg, 17.9 µmol, 2.00 equiv.) were added to an NMR tube with J. Young valve, benzene-d_6 (0.6 mL) was added, and the mixture was heated to 50°C. After six days at this temperature a mixture of products in varying concentrations was present: [{(^{Mes}nacnac)Mg}$_2$] **1c**, [(^{Mes}nacnac)Li] **5c**, [{Ph$_2$P(NDip)$_2$}MgMg(^{Mes}nacnac)] **7c**, [({Ph$_2$P(NDip)$_2$}Mg)$_2$] **2** and [{Ph$_2$P(NDip)$_2$}Li] **6**. Over time a magnesium mirror was deposited onto the inside of the NMR tube from thermal decomposition of [LMgMgL'] to [LMgL']. Heating the solution for longer only led to further decomposition.

1.3.3 Reaction of [({Ph$_2$P(NDip)$_2$}Mg)$_2$] 2 with [(^{Xyl}nacnac)Li] 5d: formation of [{Ph$_2$P(NDip)$_2$}MgMg(^{Xyl}nacnac)] 7d

[({Ph$_2$P(NDip)$_2$}Mg)$_2$] **2** (10.0 mg, 8.93 µmol) and [(^{Xyl}Nacnac)Li] **5d** (5.6 mg, 17.9 µmol, 2.01 equiv.) were added to an NMR tube with J. Young valve, benzene-d_6 (0.6 mL) was added, and the mixture was heated to 50°C. The reaction mixture changed slowly over time towards an equilibrium. After 39 days at this temperature a mixture of products was observed containing: [{(^{Xyl}nacnac)Mg}$_2$] **1d**, [(^{Xyl}nacnac)Li] **5d**, [{Ph$_2$P(NDip)$_2$}MgMg(^{Xyl}nacnac)] **7d**, [({Ph$_2$P(NDip)$_2$}Mg)$_2$] **2** and [{Ph$_2$P(NDip)$_2$}Li] **6**. Over time a magnesium mirror was deposited onto the inside of the NMR tube from partial thermal decomposition of [LMgMgL'] to [LMgL'] complexes.

NMR data for **[{Ph$_2$P(NDip)$_2$}MgMg(^{Xyl}nacnac)] 7d**: ^{1}H NMR (499.9 MHz, benzene-d_6, 295 K,) δ = 1.00 (d, J_{HH} = 6.9 Hz, 24H; ^{NPN}CH(CH_3)$_2$), 1.56 (s, 6H; ^{Xyl}NCCH_3), 2.08 (s, 12H; ^{Xyl}*o*-CH_3), 3.58 (sept, J_{HH} = 6.9 Hz, 4H; ^{NPN}CH(CH$_3$)$_2$), 4.85 (s, 1H; ^{Xyl}γ-CH), 6.79-7.13 (m, 18H; Ar-H), 7.26-7.34 (m, 4H; ^{NPN}Ph-H); ^{31}P NMR (202.4 MHz, benzene-d_6, 295 K) δ = 5.93.

1.4 Reactions of [({$Ph_2P(NDip)_2$}Mg)$_2$] 2 with C_{60}

[({$Ph_2P(NDip)_2$}Mg)$_6$$C_{60}$] 8

A mixture of C_{60} (4.5 mg, 6.22 µmol) and [({$Ph_2P(NDip)_2$}Mg)$_2$] **2** (20.9 mg, 18.65 µmol, 3.00 equiv.) were added to an NMR tube with J. Young valve, and toluene-d_8 (0.6 mL) was added giving a black-brown reaction mixture. ^{1}H and ^{31}P{^{1}H} NMR spectra show full conversion of **2** to [({$Ph_2P(NDip)_2$}Mg)$_6$$C_{60}$] **8** after approximately six days at room temperature. (N.B.: A similar reaction performed in benzene-d_6 required 2-3 weeks for completion.) Black-brown crystals of a solvate of **8** suitable for X-ray crystallographic analysis were grown from a concentrated *n*-pentane solution.

Preparative scale: Toluene (20 mL) was added to a mixture of [({$Ph_2P(NDip)_2$}Mg)$_2$] **2** (107.0 mg, 95.5 µmol, 2.99 equiv.) and C_{60} (23.0 mg, 31.9 µmol) and the black-brown mixture was vigorously stirred at room temperature for two days. The resulting solution was concentrated to *ca.* 2 mL and layered with *n*-pentane (15 mL). After allowing to diffuse slowly over three days, the brown precipitate of [({$Ph_2P(NDip)_2$}Mg)$_6$$C_{60}$] **8** was collected by filtration and dried under vacuum. Yield = 64.5 mg (50%); ^{1}H NMR (499.9 MHz, toluene-d_8, 373K) δ = 0.95 (d, J = 5.5 Hz, 144H; CH(CH_3)$_2$), 3.59 (sept, J = 7.0 Hz, 24H; CH(CH$_3$)$_2$), 6.89-6.99 (m, 48H; Ar-H), 7.03-7.07 (m, 24H; Ar-H), 7.25-7.32 (m, 24H; Ph-H); ^{13}C{^{1}H} NMR (125.7 MHz, toluene-d_8, 373 K) δ = 24.4 (br. s, CH(CH$_3$)$_2$), 30.2 (CH(CH$_3$)$_2$), 124.1 (d, J = 2.3 Hz; Ar-C), 124.3 (d, J = 3.0 Hz; Ar-C), 128.2 (Ar-C), 131.2 (d, J = 2.7 Hz; Ar-C), 132.9 (d, J = 8.4 Hz; Ar-C), 135.8 (d, J = 95.5 Hz; Ar-C), 140.9 (d, J = 3.2 Hz; Ar-C), 146.9 (d, J = 5.5 Hz; Ar-C), 155.3 (C_{60}); N.B.: the NMR spectra also contain resonances for *n*-hexane that was present from the crystallisation of [({$Ph_2P(NDip)_2$}Mg)$_2$] **2**. ^{31}P{^{1}H} NMR (202.4 MHz, toluene-d_8, 295 K) δ = 9.70 (s); N.B.: NMR spectra recorded at room temperature show some very broad resonances for the methyl groups. ^{1}H NMR (499.9 MHz, benzene-d_6, 293 K) δ = ca. 0.7-1.3 (vbr., 144H, CH(CH_3)$_2$), 3.72 (sept, J = 6.8 Hz, 24H; CH(CH$_3$)$_2$), 6.78-7.13 (m, 60H; Ar-H), 7.18 (s, 12H; Ar-H), 7.31-7.37 (m, 24H; Ar-H); ^{13}C{^{1}H} NMR (125.7 MHz, benzene-d_6, 293 K) δ = 22-27 (vbr., CH(CH$_3$)$_2$) 29.9 (CH(CH$_3$)$_2$), 123.9 (two overlapping d, J $\approx$ 3.5 and 2.1 Hz; 2 Ar-C), 127.97 (Ar-C), 128.4 (Ar-C), 131.0 (d, J = 2.3 Hz; Ar-C), 132.4 (d, J = 8.3 Hz; Ar-C), 134.7 (d, J = 95.6 Hz; Ar-C), 140.4 (d, J = 3.0 Hz; Ar-C), 146.3 (d, J = 5.4 Hz; Ar-C), 154.9 (C_{60}); ^{31}P{^{1}H} NMR (202.4 MHz, benzene-d_6, 293 K) δ = 9.77 (s); IR (nujol), $\tilde{v}$/cm^{-1}: 2957 (m), 2921 (w), 2864 (w), 1589 (w), 1456 (m), 1433 (s), 1381 (m), 1358 (m), 1329 (m), 1254 (m), 1111 (s), 1055 (w), 1043 (w), 997 (w), 975 (w), 905 (m), 818 (m), 789 (s), 743 (s), 694 (s), 569 (w), 505 (m); M.p.: decomposition 216-220°C; elemental analysis: calculated for $C_{276}H_{264}Mg_6N_{12}P_6$: C, 81.23; H, 6.52; N, 4.12%; found: C, 80.95; H, 6.65; N 3.96%.

2 NMR spectroscopy

2.1 General considerations

Unless stated otherwise, NMR spectra were recorded in deuterated benzene. Chemical shifts are given in ppm. Resonance labels in blue correspond to the compound in question, whilst grey labels represent resonances belonging to by-products/impurities in solution. Some resonances in spectra of reaction mixtures are labelled as follows; 'DipMg', 'DepMg', 'MesMg' and 'XylMg' correspond to complexes **1a-d** respectively, whilst 'Dip/DepMg', 'Dip/MesMg', 'Dep/MesMg', 'Dep/XylMg' and 'Mes/XylMg', or vice versa ('Dep/DipMg' etc.), correspond to scrambled products **4ab** to **4cd**, respectively. Similarly, lithium complexes **5c** and **5d** are represented as 'MesLi' and 'XylLi' respectively. Complexes containing the $\{Ph_2P(NDip)_2\}$ ligand fragment are denoted as 'L1'; *i.e.* L1Mg corresponds to **2**, for example, whilst L1/MesMg corresponds to **7c**. HMB = hexamethylbenzene (used as an internal standard for some reactions herein). Note that in several reactions not all species may be soluble at all times, *i.e.* they may not be fully dissolved (e.g. **1c**). Further information has been provided in the Figure captions.

2.2 NMR spectra of mixed magnesium(I) dimers [(^{Ar}nacnac)MgMg($^{Ar'}$nacnac)] 4 from scrambling reactions

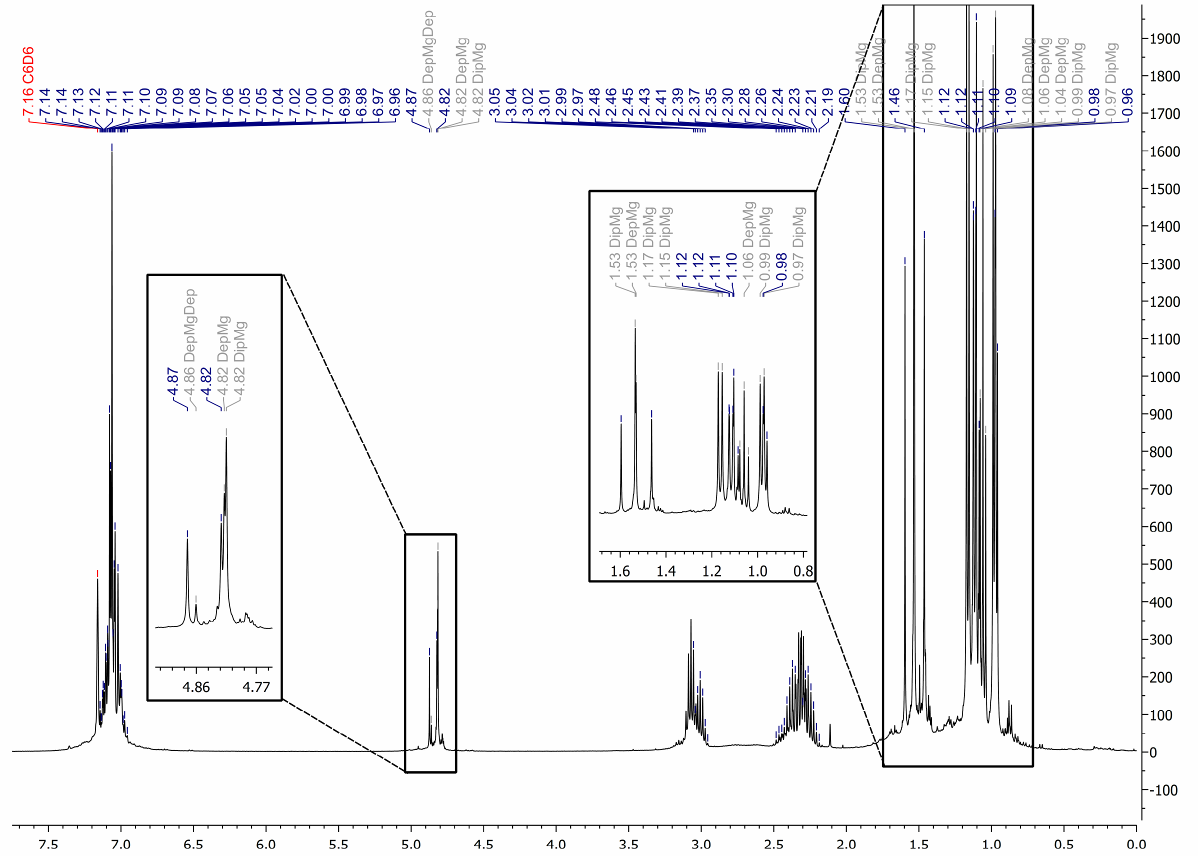

Figure S1. ^{1}H NMR spectrum (499.9 MHz, 295 K) of the equilibrium between [{(^{Dip}nacnac)Mg}$_2$] **1a**, [{(^{Dep}nacnac)Mg}$_2$] **1b** and [(^{Dip}nacnac)MgMg(^{Dep}nacnac)] **4ab**, established after heating the mixture of reactants, **1a** and **1b**, in the presence of catalytic C_{60} (11 mol%), for seven days at 70°C.

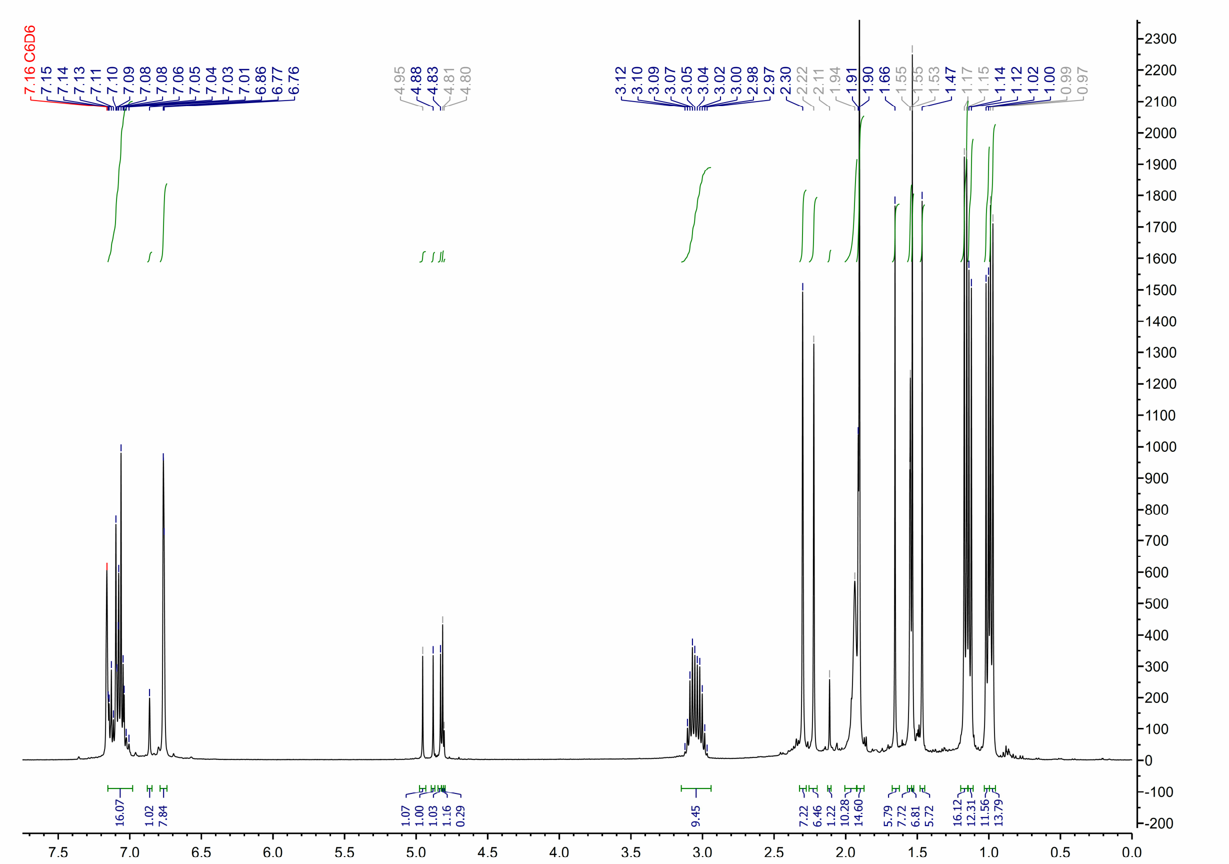

Figure S2. ^{1}H NMR spectrum (499.9 MHz, 295 K) of the mixture of [{(^{Dip}nacnac)Mg}$_2$] **1a**, [{(^{Mes}nacnac)Mg}$_2$] **1c**, [(^{Dip}nacnac)MgMg(^{Mes}nacnac)] **4ac**, and other species after storing a mixture of reactants, **1a** and **1c**, for 53 days at room temperature. Note that a significant quantity of the magnesium(II) complex [(^{Mes}nacnac)$_2$Mg] (CH singlet at δ 4.95 ppm) and Mg metal formed.

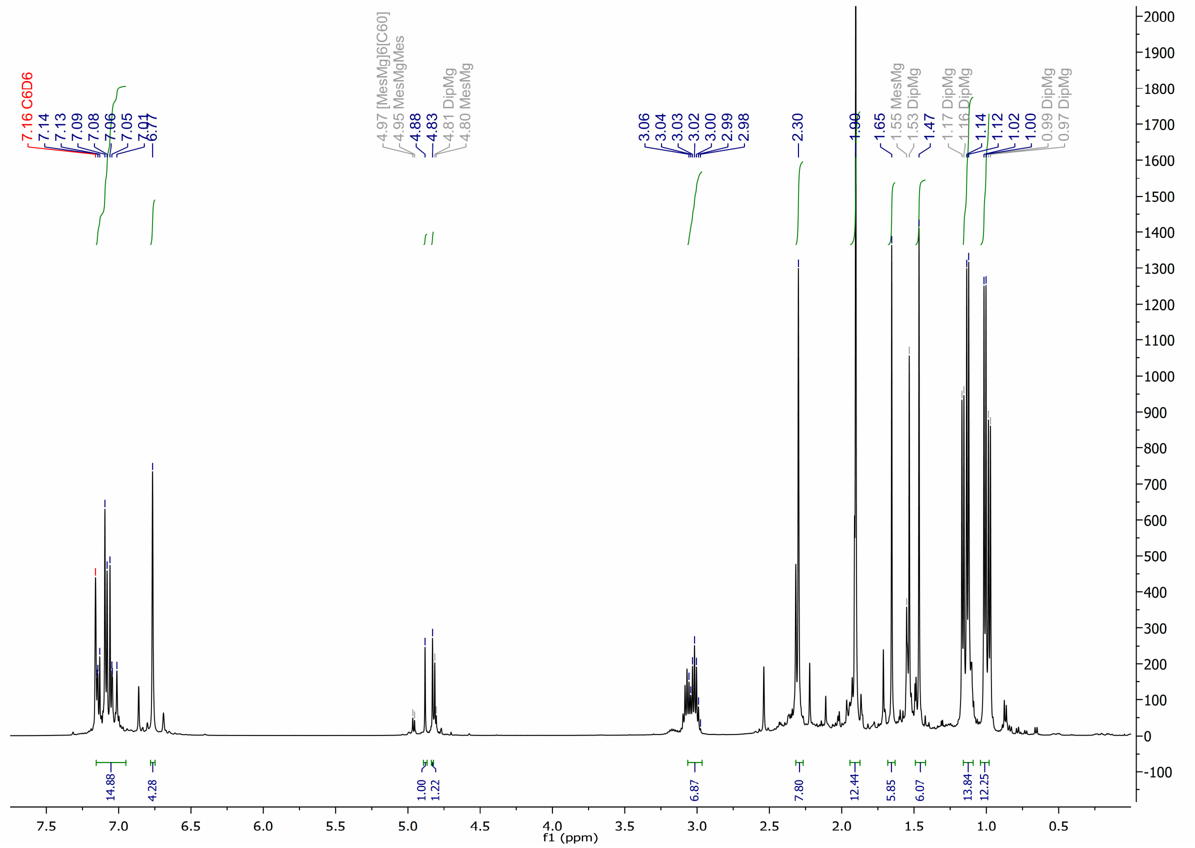

Figure S3. ^{1}H NMR spectrum (499.9 MHz, 295 K) of the reaction mixture resulting from [{(^{Dip}nacnac)Mg}$_2$] **1a**, [{(^{Mes}nacnac)Mg}$_2$] **1c** and catalytic C_{60} (10 mol%) after 59 days at room temperature, forming [(^{Dip}nacnac)MgMg(^{Mesn}nacnac)] **4ac**, and other species. Note the significantly reduced quantity of [(^{Mes}nacnac)$_2$Mg] (CH singlet at δ 4.95 ppm) in comparison to spectrum Figure S2 from decomposition reactions. Less Mg metal, compared to the previous experiment, had formed from decomposition by visual inspection.

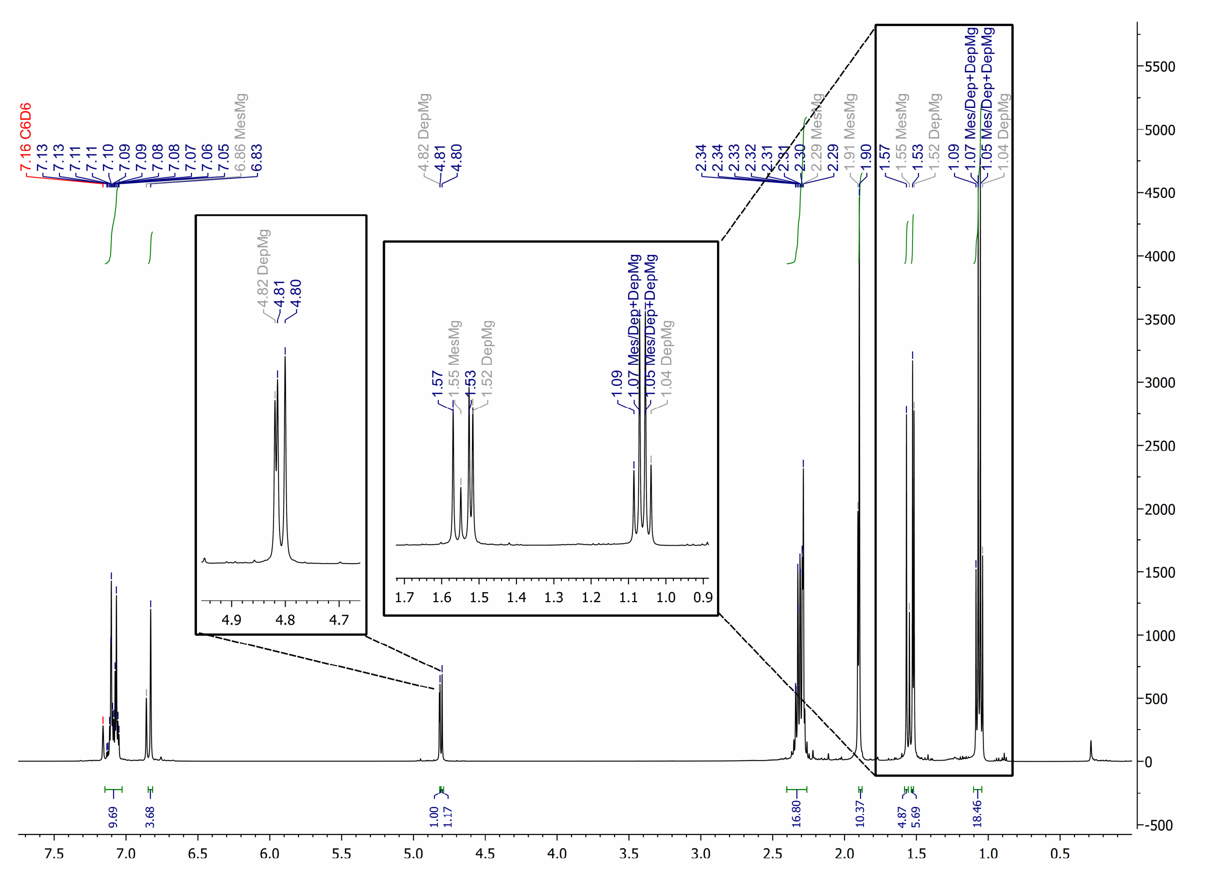

Figure S4. ^{1}H NMR spectrum (499.9 MHz, 295 K) of the resting equilibrium between [{(^{Dep}nacnac)Mg}$_2$] **1b**, [{(^{Mes}nacnac)Mg}$_2$] **1c** and [(^{Dep}nacnac)MgMg(^{Mes}nacnac)] **4bc**, established after storing the mixture of reactants, **1b** and **1c**, for 22 h at room temperature.

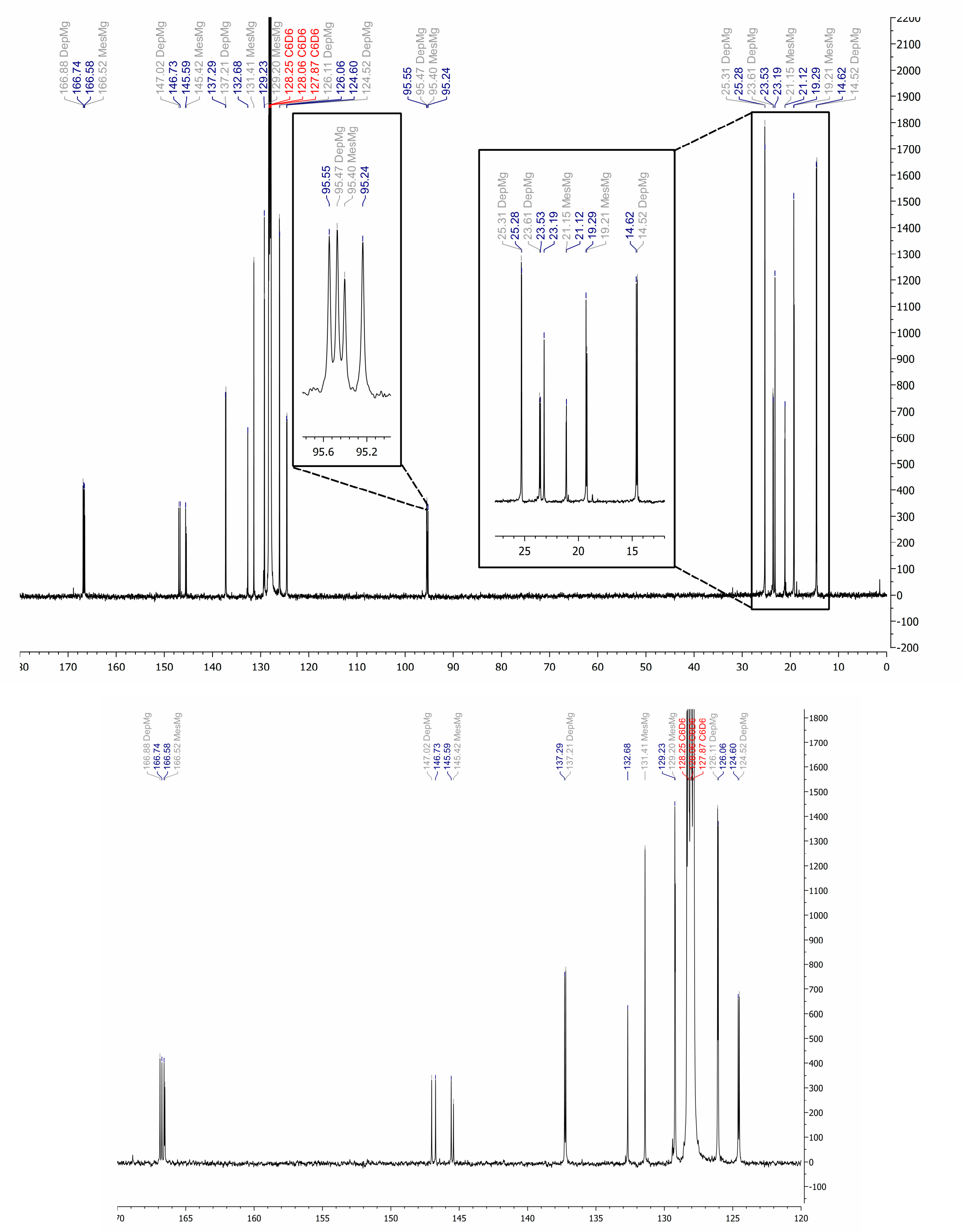

Figure S5. $^{13}C\{^{1}H\}$ NMR spectrum (125.7 MHz, 295 K) of the resting equilibrium between $[\{(^{Dep}nacnac)Mg\}_2]$ **1b**, $[\{(^{Mes}nacnac)Mg\}_2]$ **1c** and $[(^{Dep}nacnac)MgMg(^{Mes}nacnac)]$ **4bc**.

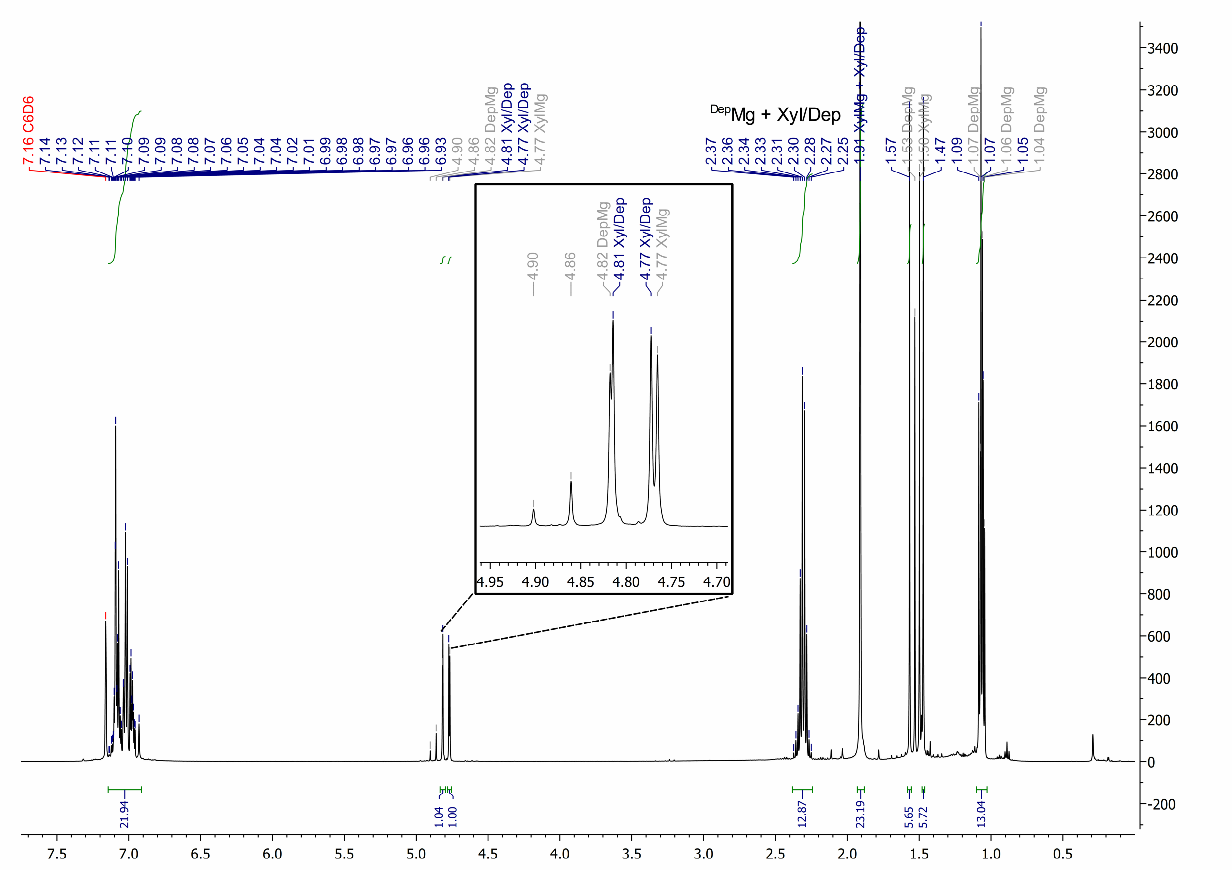

Figure S6. ^{1}H NMR spectrum (499.9 MHz, 295 K) of the resting equilibrium between [{(^{Dep}nacnac)Mg}$_2$] **1b**, [{(^{Xyl}nacnac)Mg}$_2$] **1d** and [(^{Dep}nacnac)MgMg(^{Xyl}nacnac)] **4bd**, established after storing the mixture of reactants, **1b** and **1c**, for 19 h at room temperature.

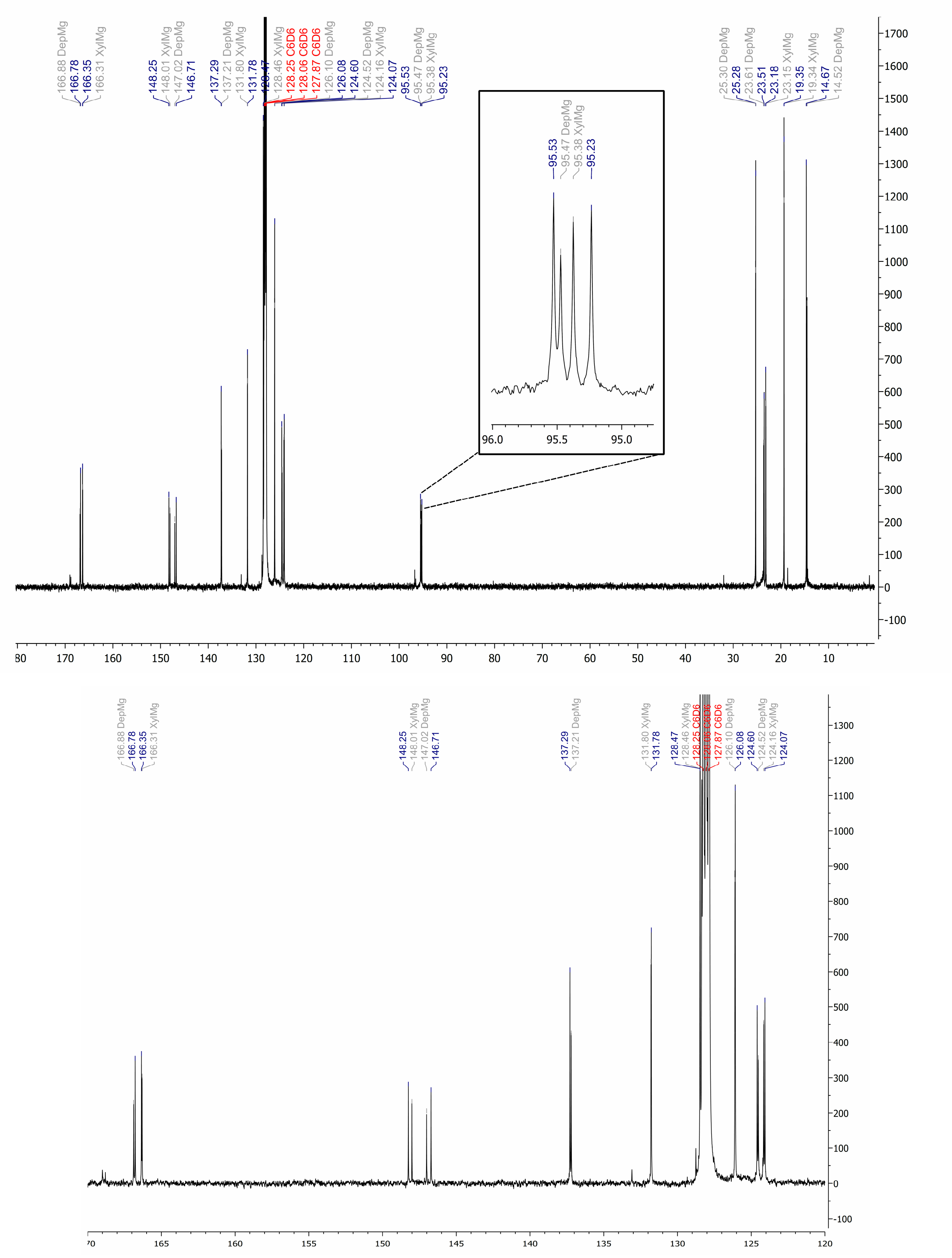

Figure S7. $^{13}C\{^1H\}$ NMR spectrum (125.7 MHz, 295 K) of the resting equilibrium between [{(^{Dep}nacnac)Mg}$_2$] **1b**, [{(^{Xyl}nacnac)Mg}$_2$] **1d** and [(^{Dep}nacnac)MgMg(^{Xyl}nacnac)] **4bd**.

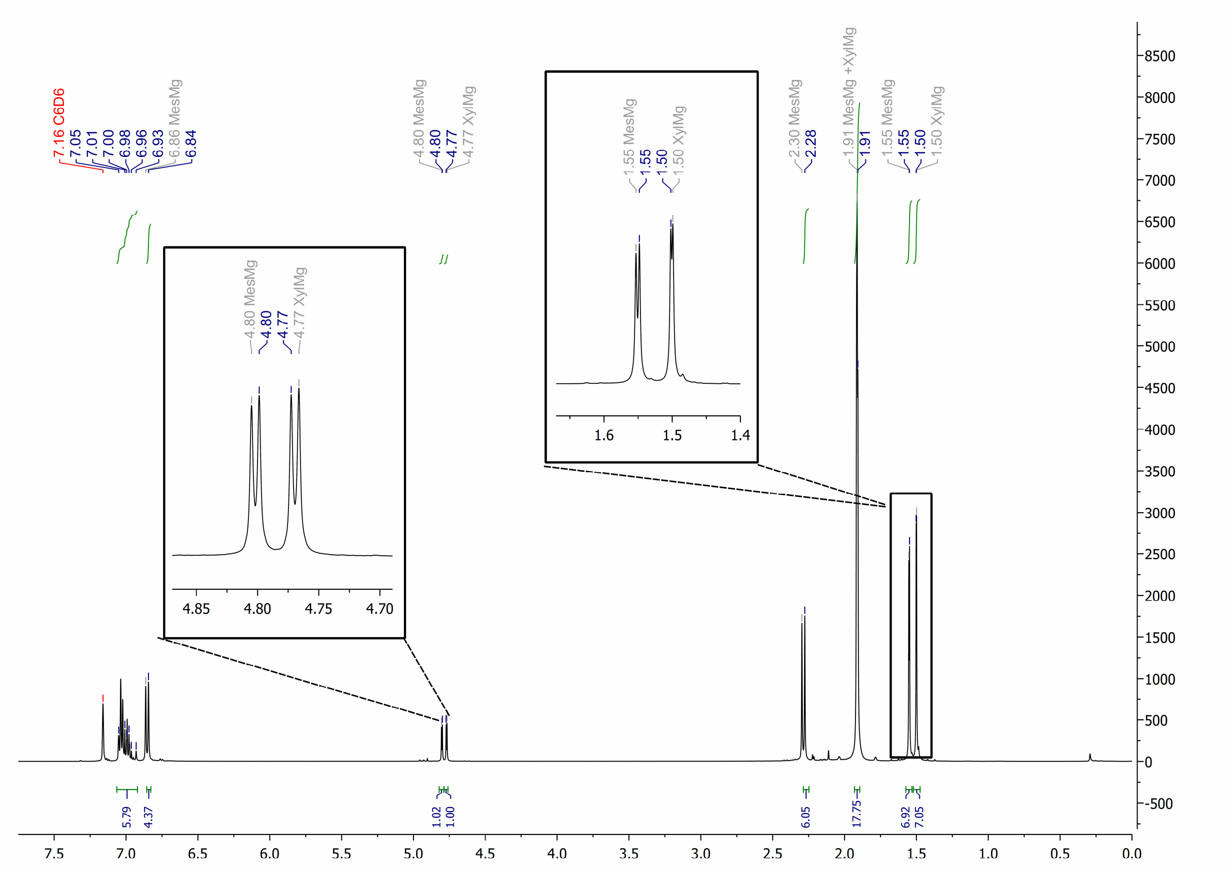

Figure S8. ^{1}H NMR spectrum (499.9 MHz, 295 K) of the resting equilibrium between [{(^{Mes}nacnac)Mg}$_2$] **1c**, [{(^{Xyl}nacnac)Mg}$_2$] **1d** and [(^{Mes}nacnac)MgMg(^{Xyl}nacnac)] **4cd**, established after storing the mixture of reactants, **1c** and **1d**, for circa five minutes at room temperature.

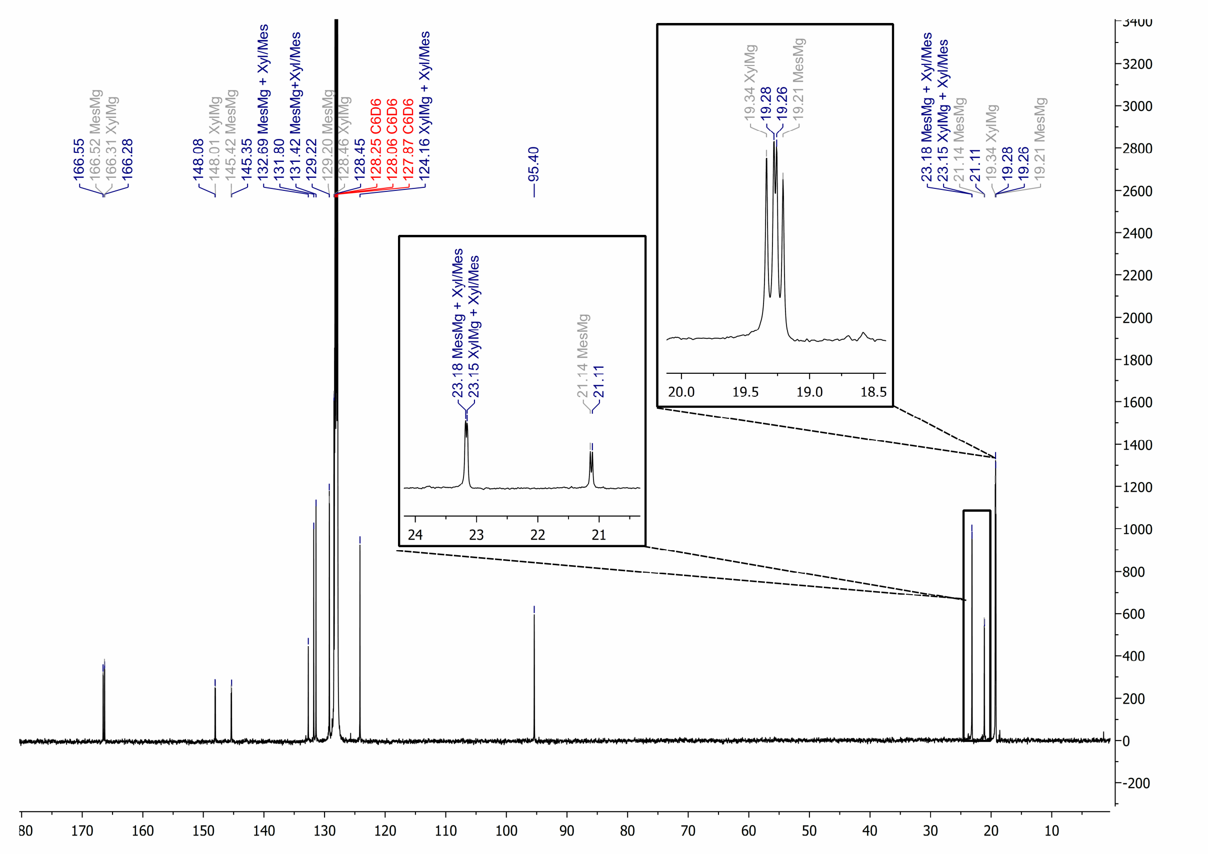

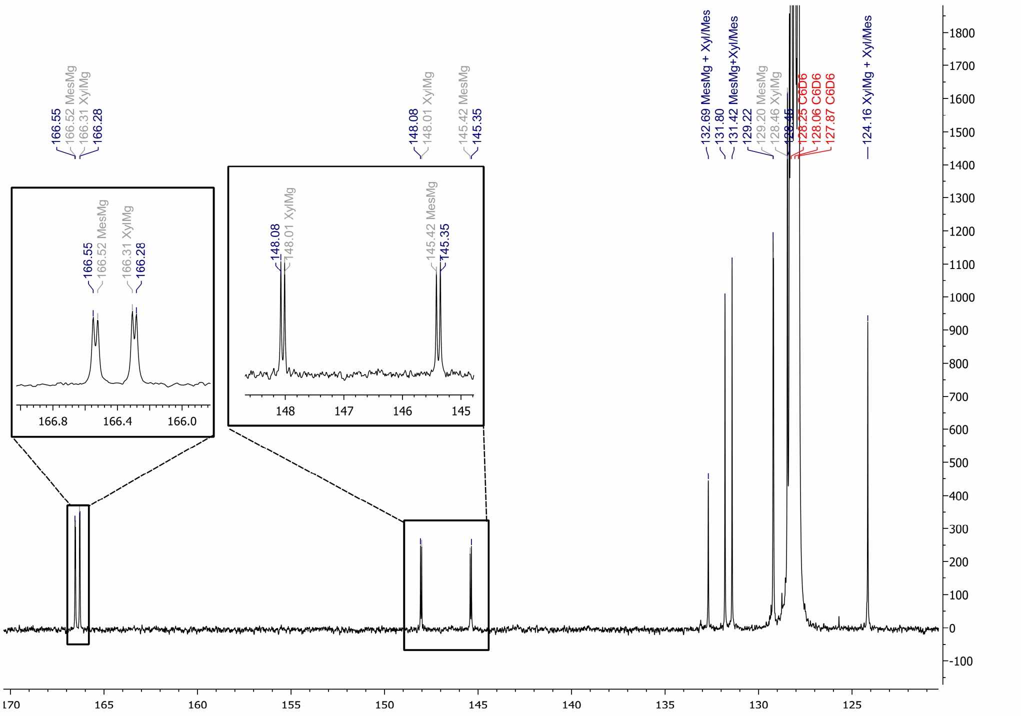

Figure S9. $^{13}C\{^{1}H\}$ NMR spectrum (125.7 MHz, 295 K, incl. zoom 120-170 ppm) of the resting equilibrium between [{(^{Mes}nacnac)Mg}$_2$] **1c**, [{(^{Xyl}Nacnac)Mg}$_2$] **1d** and [(^{Mes}nacnac)MgMg(^{Xyl}nacnac)] **4cd**.

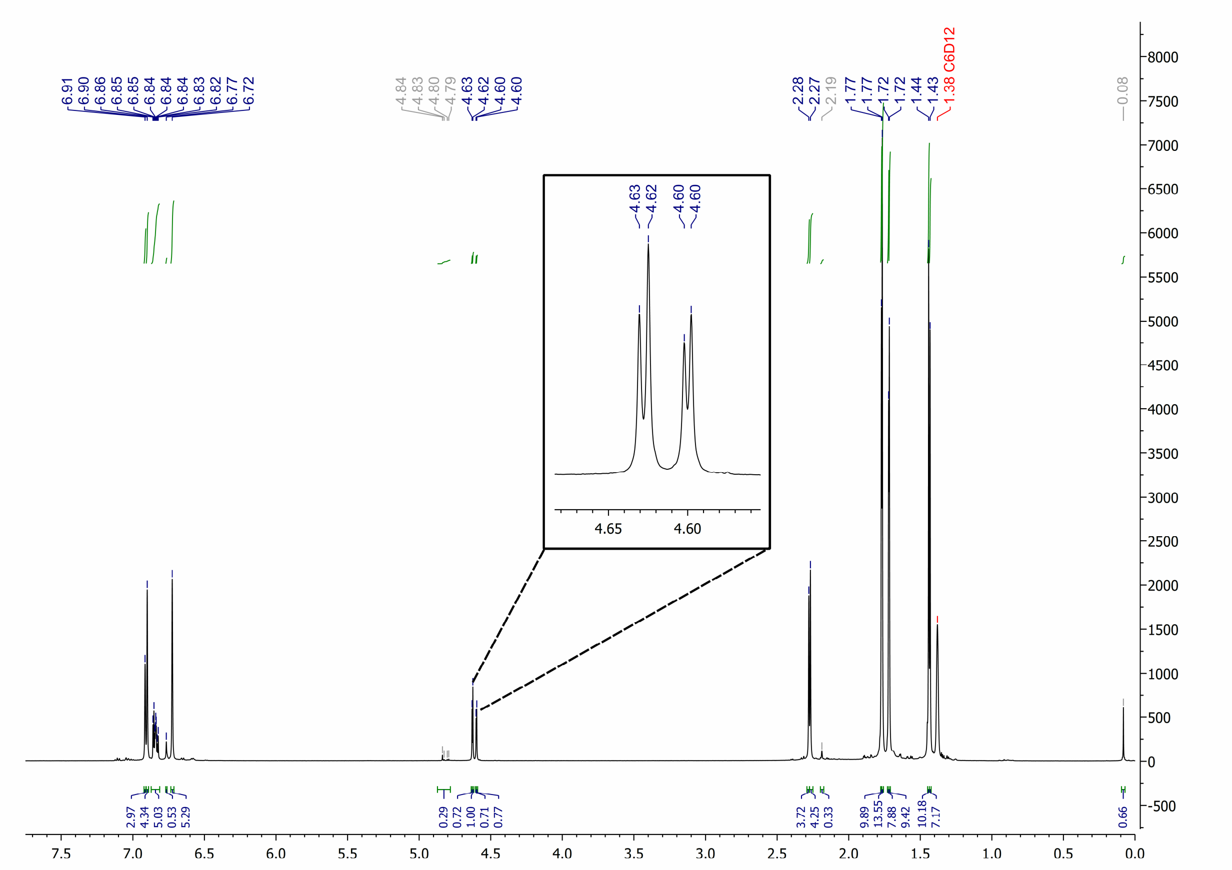

Figure S10. ^{1}H NMR spectrum (499.9 MHz, 295 K) of the resting equilibrium of [{(^{Mes}nacnac)Mg}$_2$] **1c**, [{(^{Xyl}nacnac)Mg}$_2$] **1d** and [(^{Mes}nacnac)MgMg(^{Xyl}nacnac)] **4cd** in cylcohexane-d_{12} acquired after storing the mixture of reactants, **1c** and **1d**, for circa five minutes at room temperature.

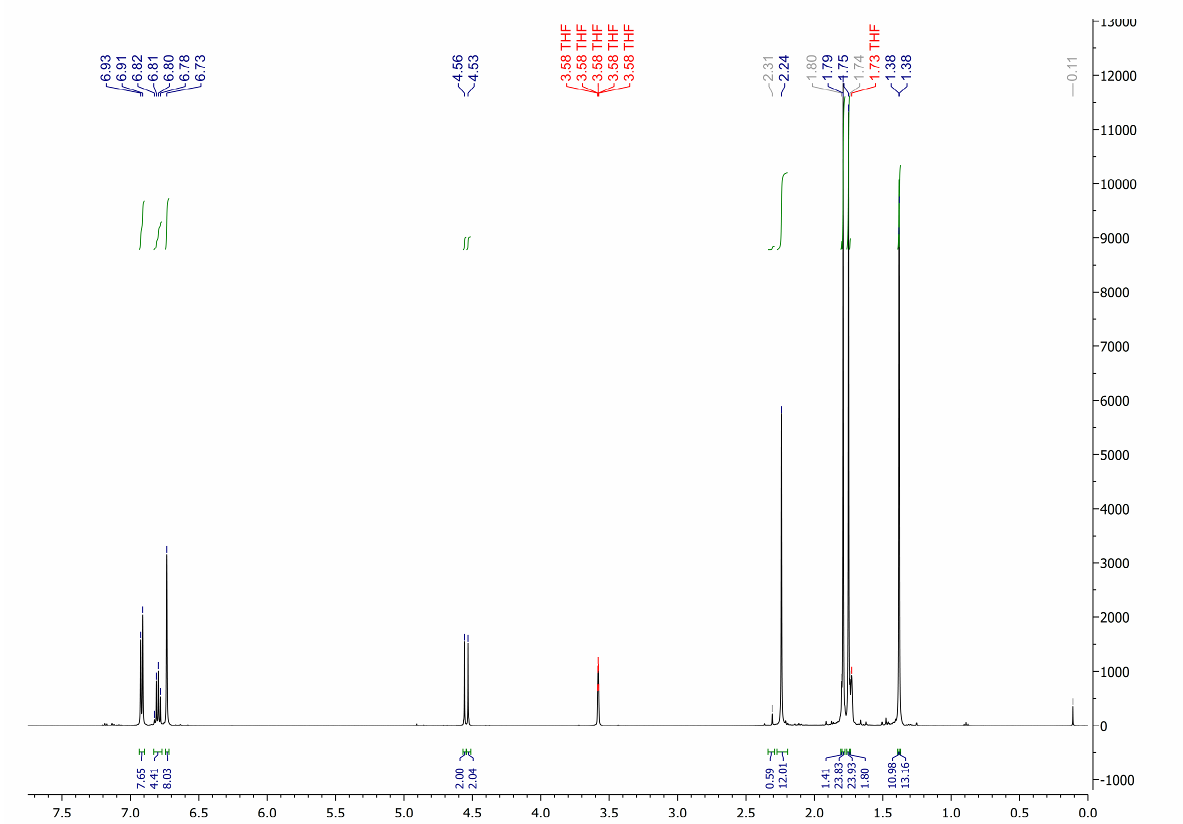

Figure S11. ^{1}H NMR spectrum (499.9 MHz, 295 K) of unscrambled [($^{\mathrm{Mes}}$nacnac)Mg(THF)-Mg(THF)($^{\mathrm{Mes}}$nacnac)] **1c-THF**, and [($^{\mathrm{Xyl}}$nacnac)Mg(THF)Mg(THF)($^{\mathrm{Xyl}}$nacnac)] **1d-THF** in THF-d_8, immediately after dissolving at room temperature.

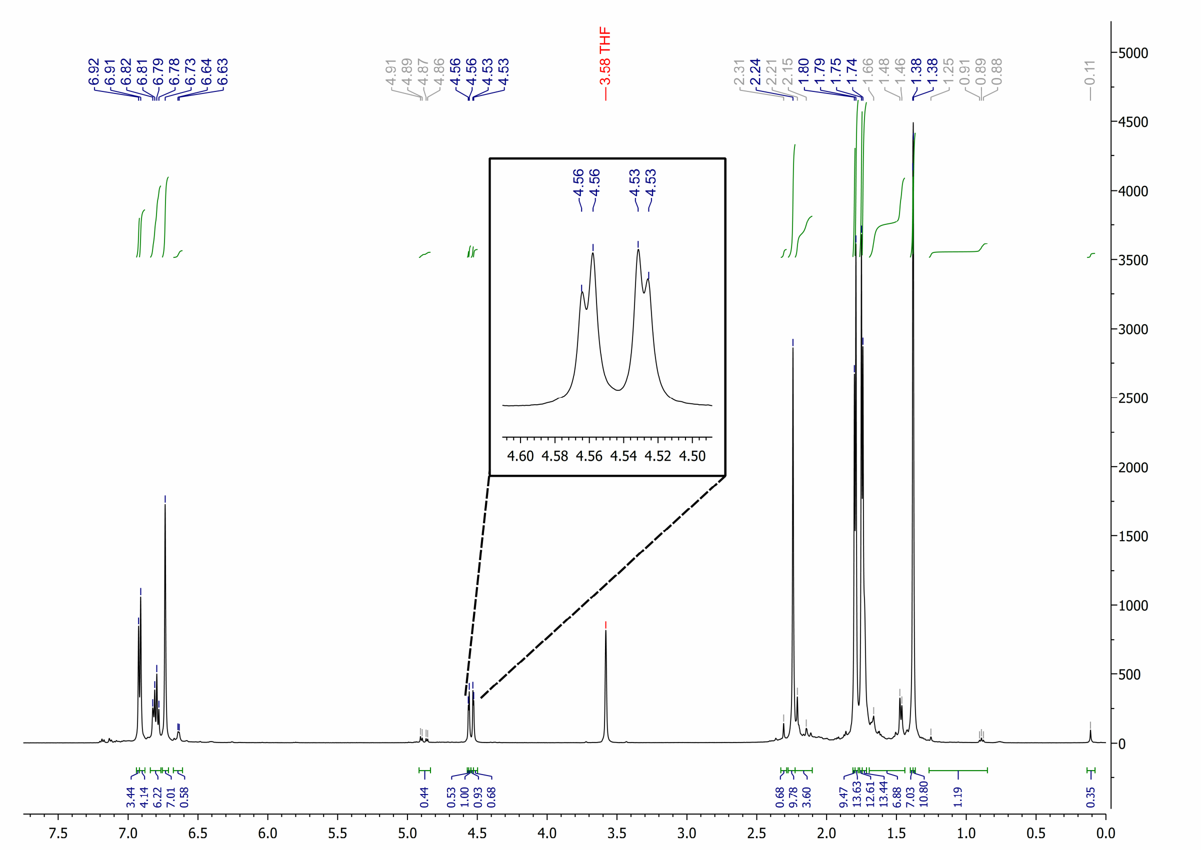

Figure S12. ^{1}H NMR spectrum (499.9 MHz, 295 K) of the "near equilibrium" between [($^{\text{Mes}}$nacnac)Mg(THF)Mg(THF)($^{\text{Mes}}$nacnac)] **1c-THF**, [($^{\text{Xyl}}$nacnac)Mg(THF)Mg(THF)($^{\text{Xyl}}$nacnac)] **1d-THF** and [($^{\text{Mes}}$nacnac)Mg(THF)Mg(THF)($^{\text{Xyl}}$nacnac)] **4cd-THF** in THF-d_8, established after heating the mixture of reactants, **1c-THF** and **1d-THF**, for 29 days at 50°C.

2.3 Ligand exchange reactions involving complexes 1-7

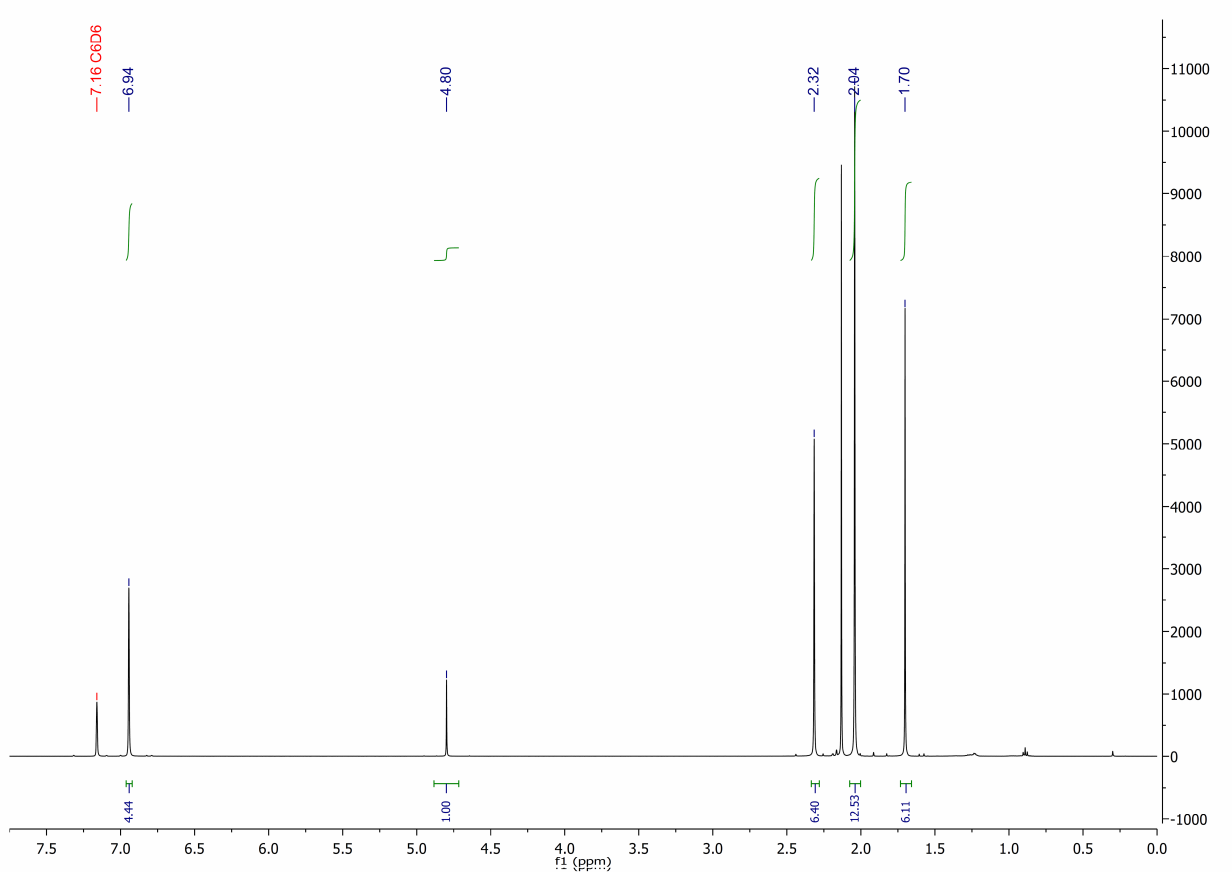

Figure S13. ^{1}H NMR spectrum (499.9 MHz, 295K) of isolated [(^{Mes}nacnac)Li] **5c**.

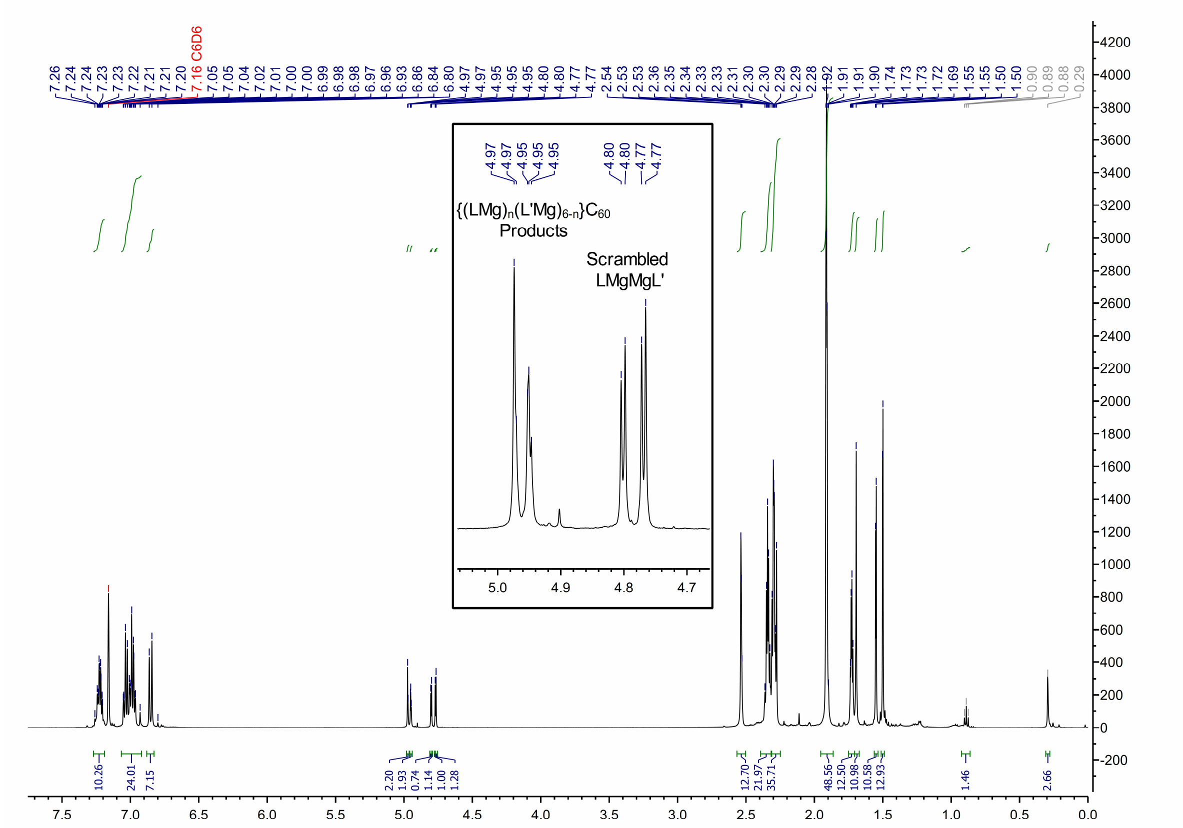

Figure S14. ^{1}H NMR spectrum (499.9 MHz, 295 K) of the reaction of [{(^{Mes}nacnac)Mg}$_6$C$_{60}$] **3c** with three equivalents of [{(^{Xyl}nacnac)Mg}$_2$] **1d** established after storing the mixture for two days at room temperature showing an approximate resting equilibrium. Insert: β-diketiminate γ-CH region with product labels shown (L and L' refer to (^{Ar}nacnac), with Ar = Mes, Xyl).

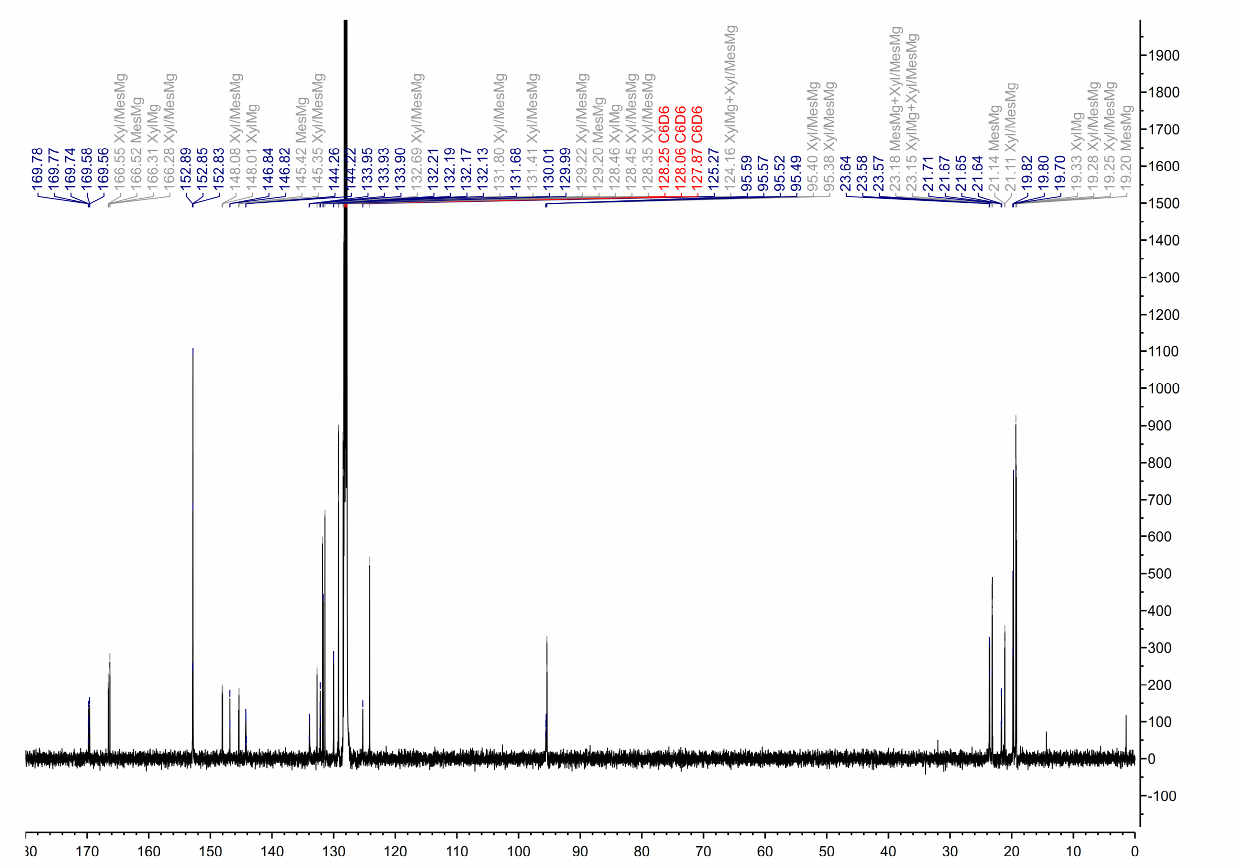

Figure S15. $^{13}C\{^1H\}$ NMR spectrum (125.7 MHz, 295 K) of the reaction of $[\{(^{Mes}nacnac)Mg\}_6C_{60}]$ **3c** with three equivalents of $[\{(^{Xyl}nacnac)Mg\}_2]$ **1d** showing a resting equilibrium (*c.f.* ^1H NMR spectrum Figure S14). Resonances labelled in grey correspond to LMgMgL' products whilst resonances labelled in blue correspond to $[\{(LMg)_n(L'Mg)_{6-n}\}C_{60}]$ complexes (L and L' refer to (^{Ar}nacnac), with Ar = Mes, Xyl).

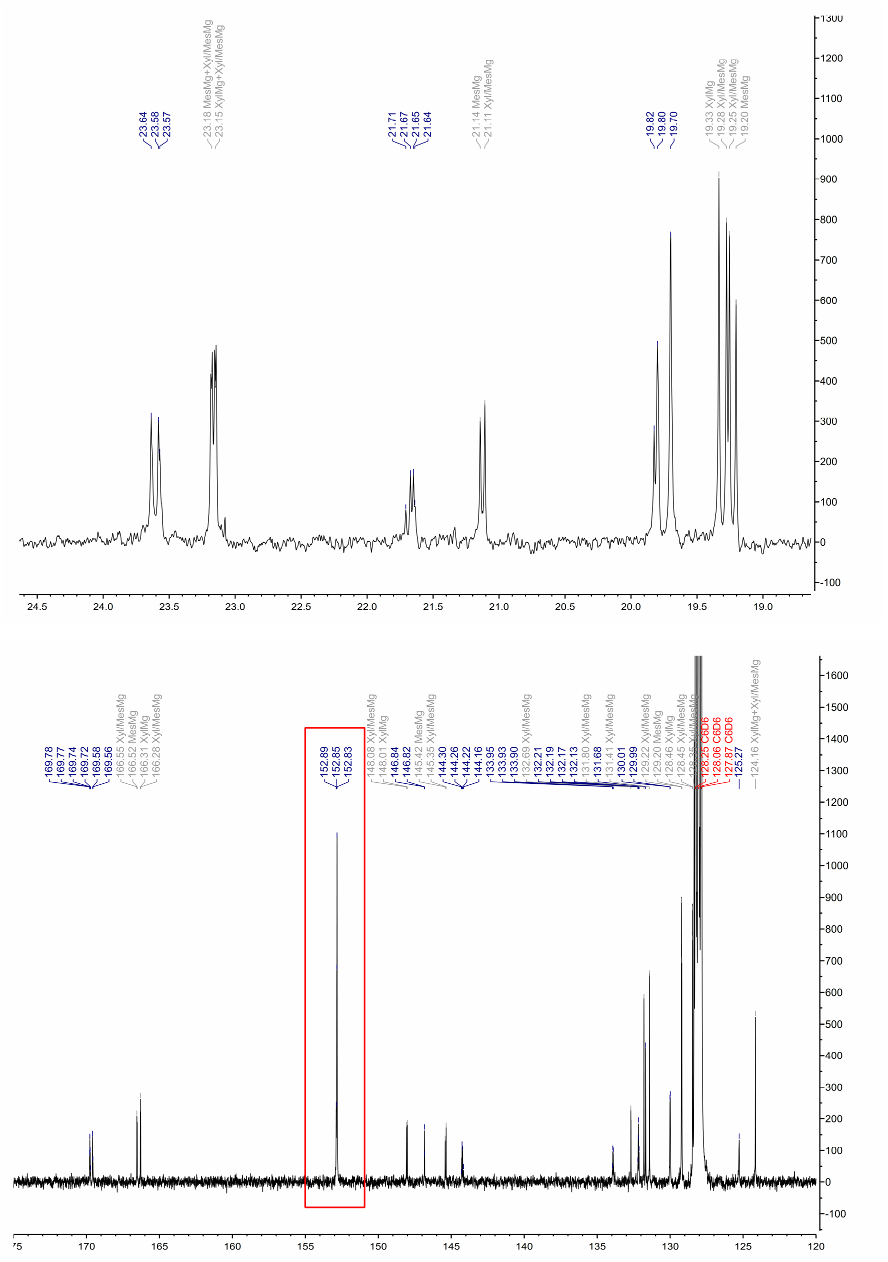

Figure S16. Excerpts of the $^{13}C\{^{1}H\}$ NMR spectrum (125.7 MHz, 295 K) in Figure S71. Resonances labelled in grey correspond to LMgMgL' products whilst resonances labelled in blue correspond to $[\{(LMg)_n(L'Mg)_{6-n}\}C_{60}]$ complexes (L and L' refer to (^{Ar}nacnac), with Ar = Mes, Xyl). Resonances within the red box display the C_{60} carbon environments and correspond exclusively to $C_{60}{}^{6-}$ fragments.

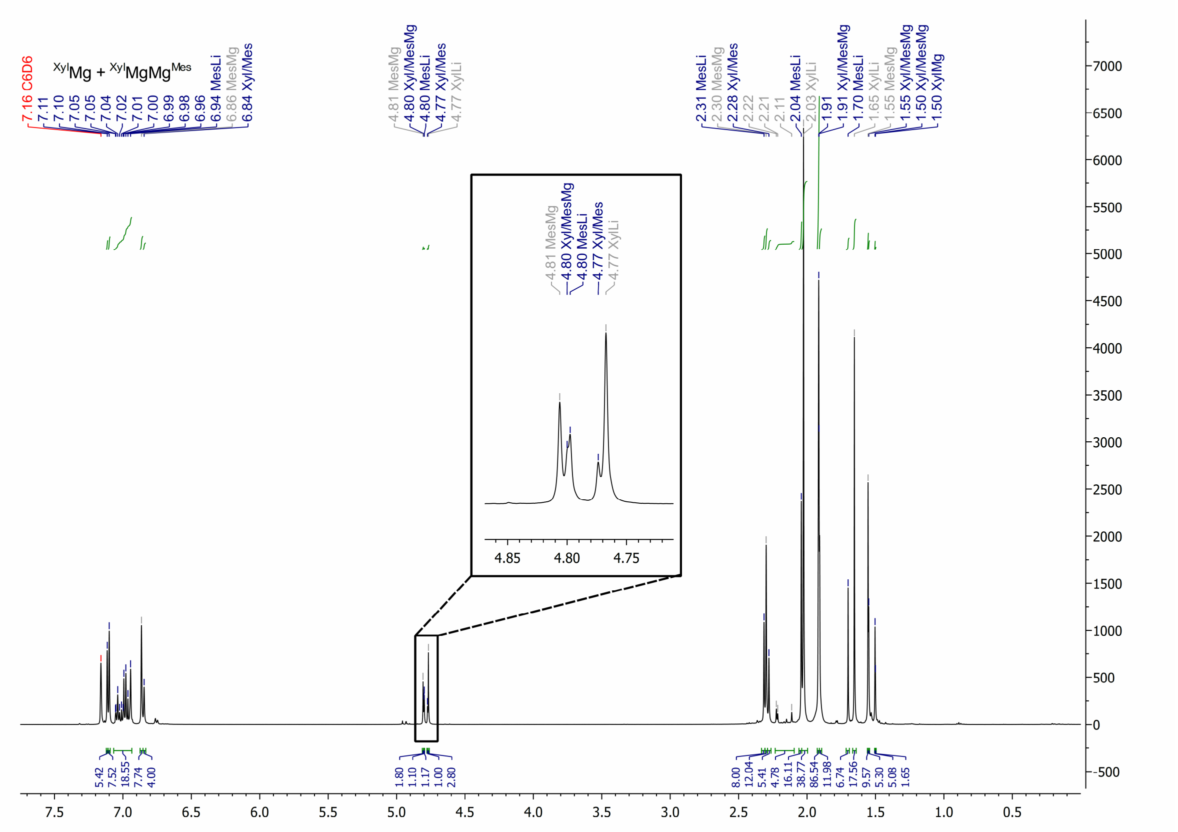

Figure S17. ^{1}H NMR (499.9 MHz, 295 K) spectrum of the reaction mixture of [{(^{Mes}nacnac)Mg}$_2$] **1c** and two equivalents of [{(^{Xyl}nacnac)Li] **5d** after heating for six days at 50°C.

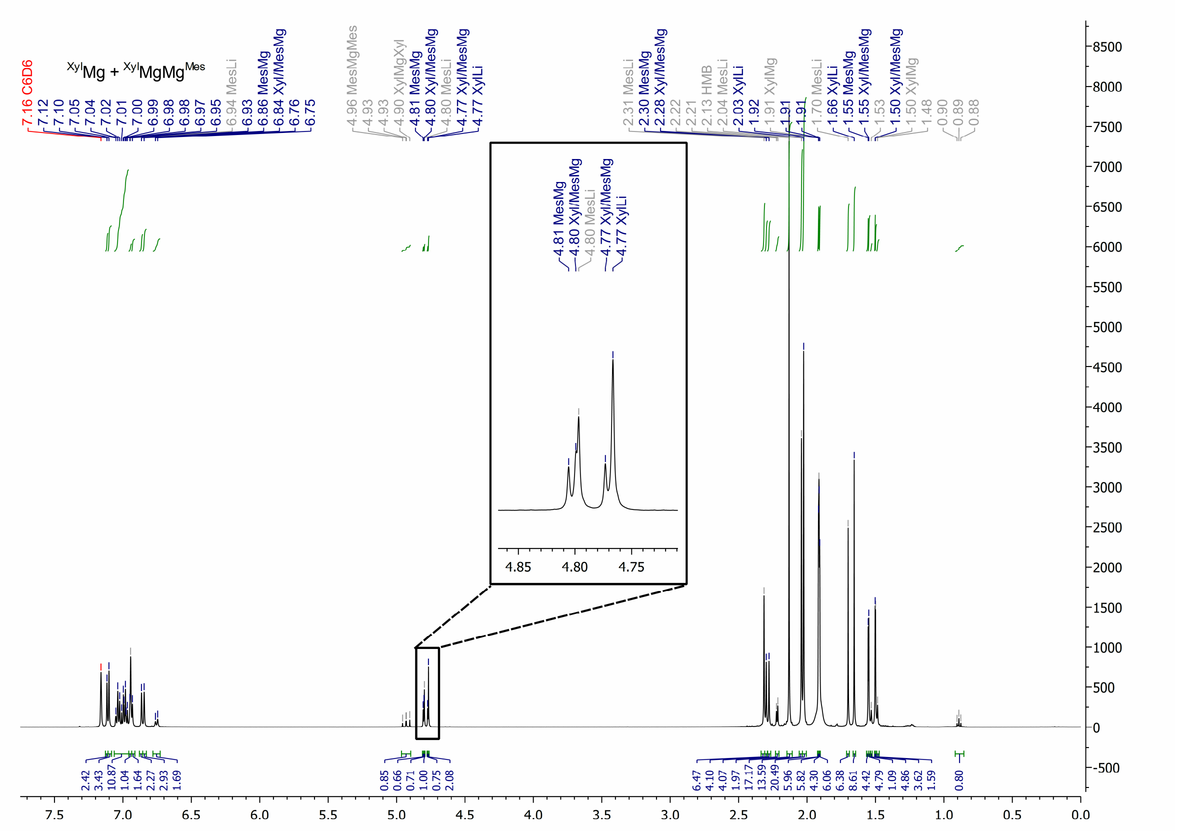

Figure S18. ^{1}H NMR spectrum (499.9 MHz, 295 K) of the reaction mixture of [{(^{Xyl}nacnac)Mg}$_2$] **1d** and two equivalents of [{(^{Mes}nacnac)Li] **5c** after five days at 50°C.

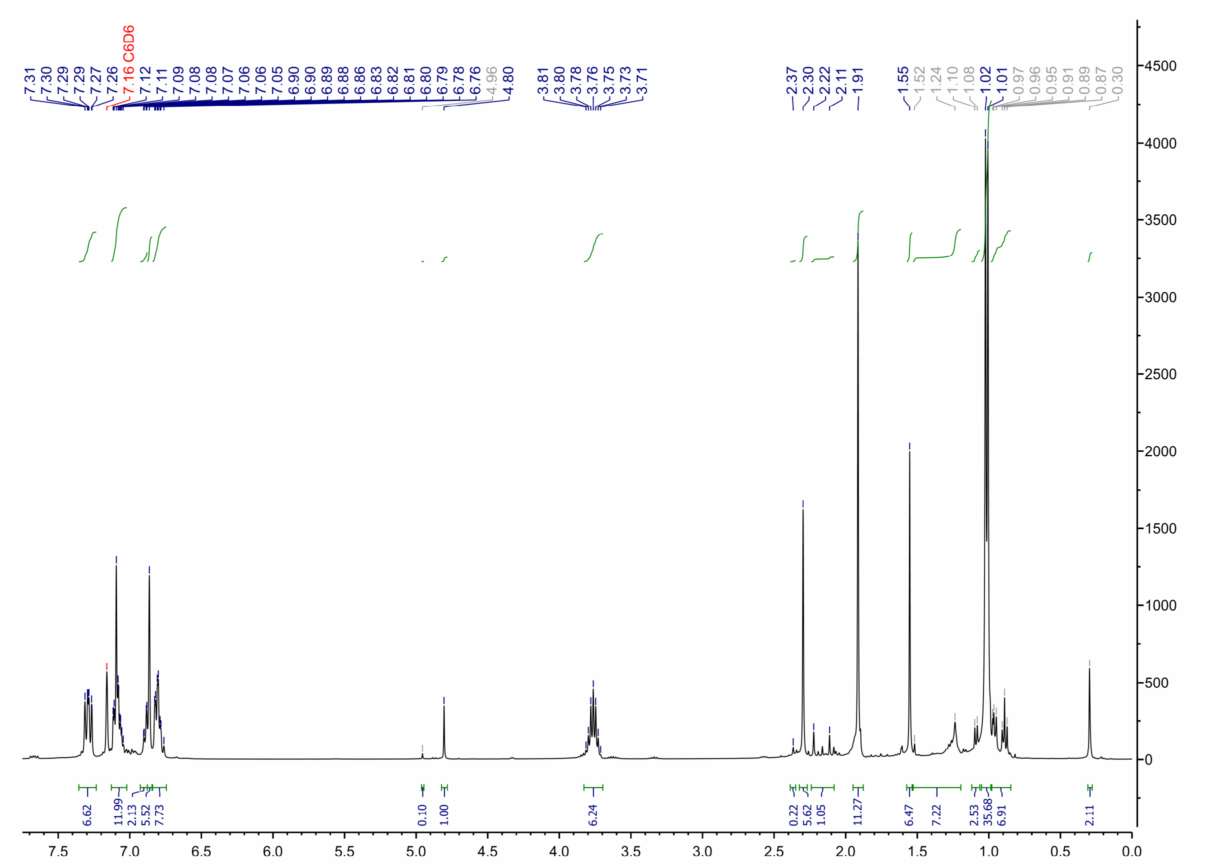

Figure S19. ^{1}H NMR spectrum (499.9 MHz, 295 K) of [{(^{Mes}nacnac)Mg}$_2$] **1c** and [({Ph$_2$P(NDip)$_2$}Mg)$_2$] **2** immediately after addition. Note: not all **1c** was fully dissolved.

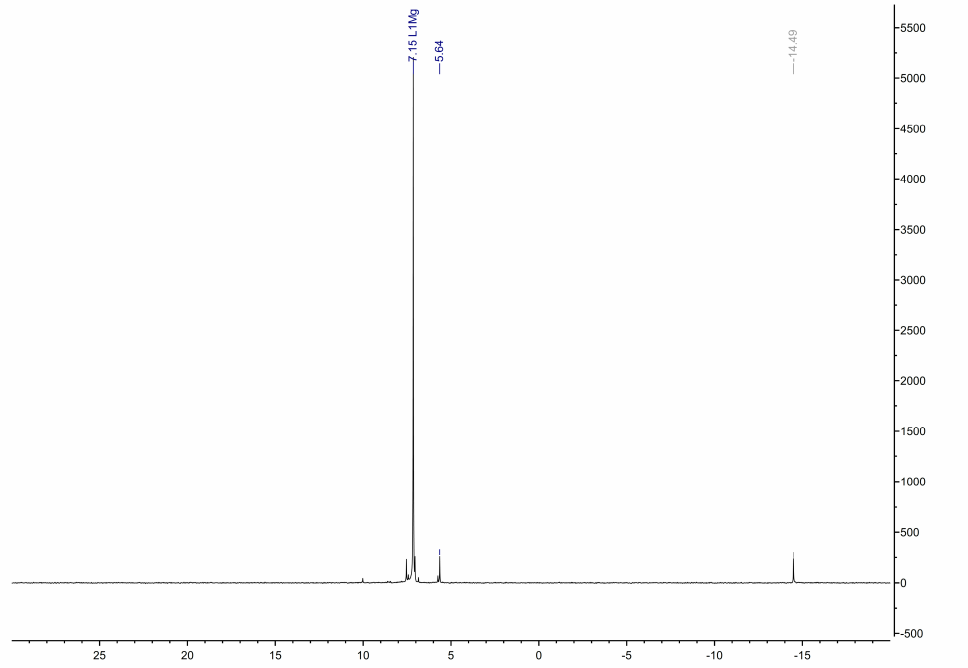

Figure S20. ^{31}P{^{1}H} NMR spectrum (202.4 MHz, 295 K) of [{(^{Mes}nacnac)Mg}$_2$] **1c** and [({Ph$_2$P(NDip)$_2$}Mg)$_2$] **2** immediately after addition.

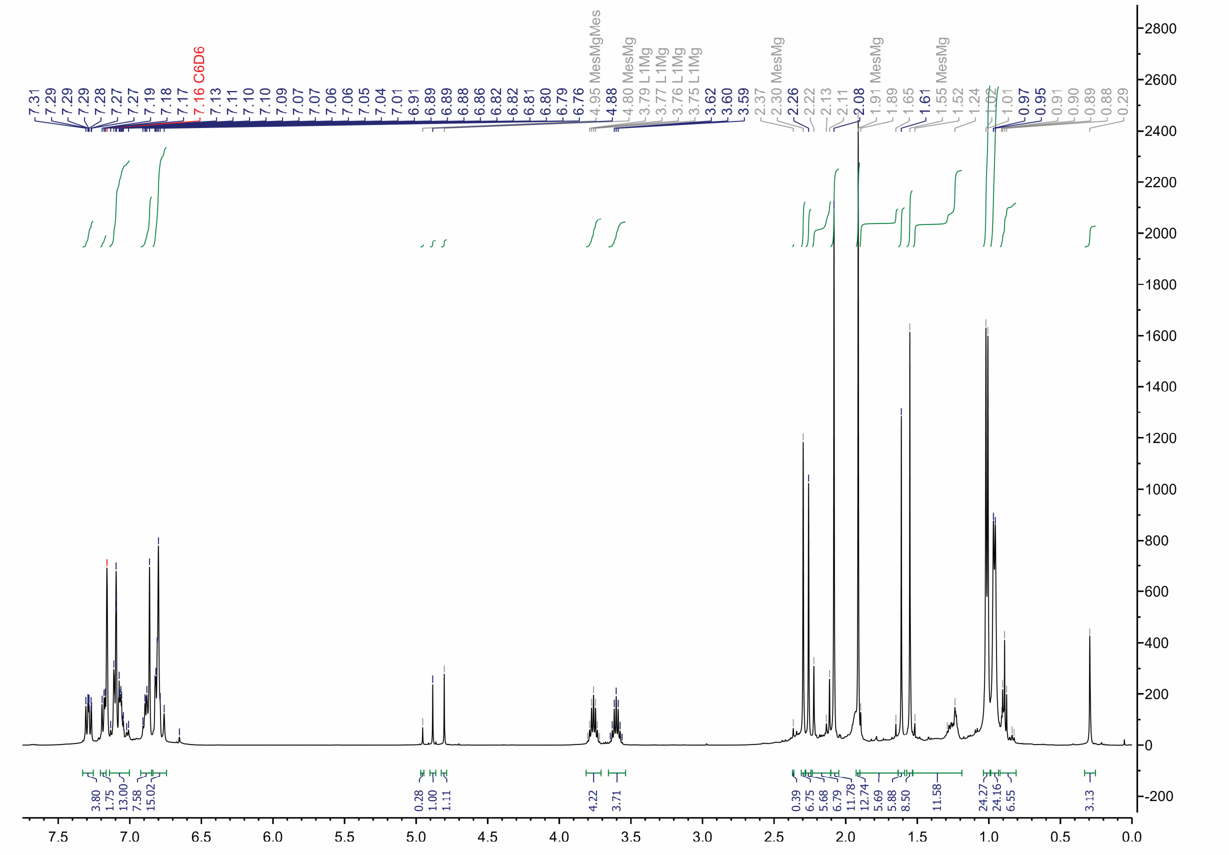

Figure S21. ^{1}H NMR spectrum (499.9 MHz, 295 K) of [{(^{Mes}nacnac)Mg}$_2$] **1c** and [({Ph$_2$P(NDip)$_2$}Mg)$_2$] **2** after ten days at room temperature. Note: the sample was now fully dissolved.

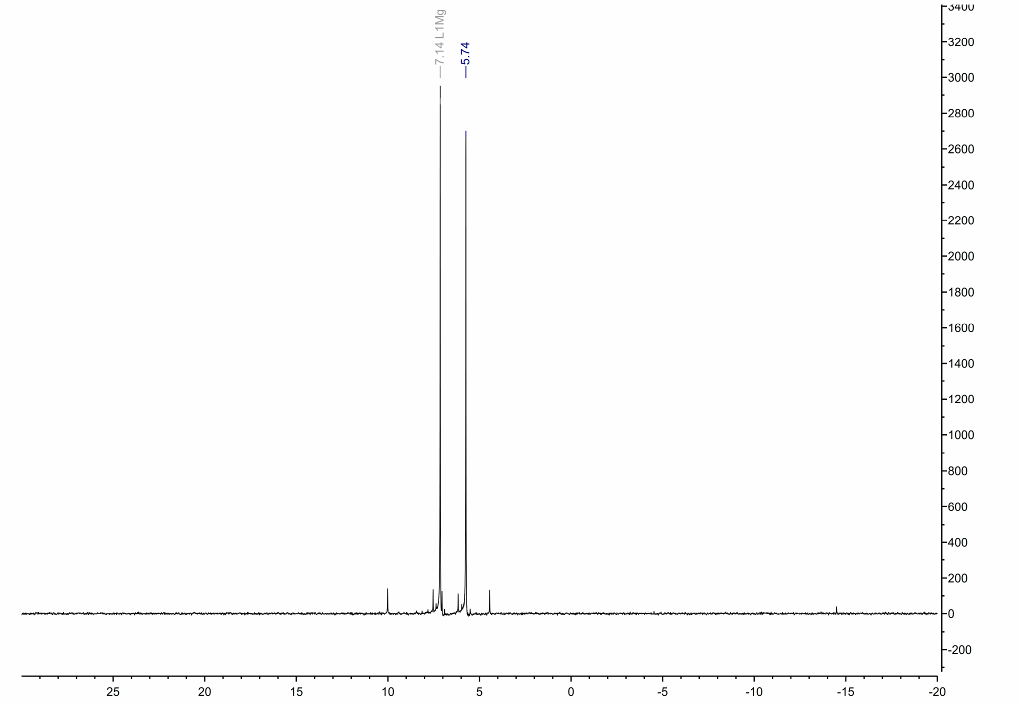

Figure S22. ^{31}P{^{1}H} NMR spectrum (202.4 MHz, 295 K) of [{(^{Mes}nacnac)Mg}$_2$] **1c** and [({Ph$_2$P(NDip)$_2$}Mg)$_2$] **2** after ten days at room temperature.

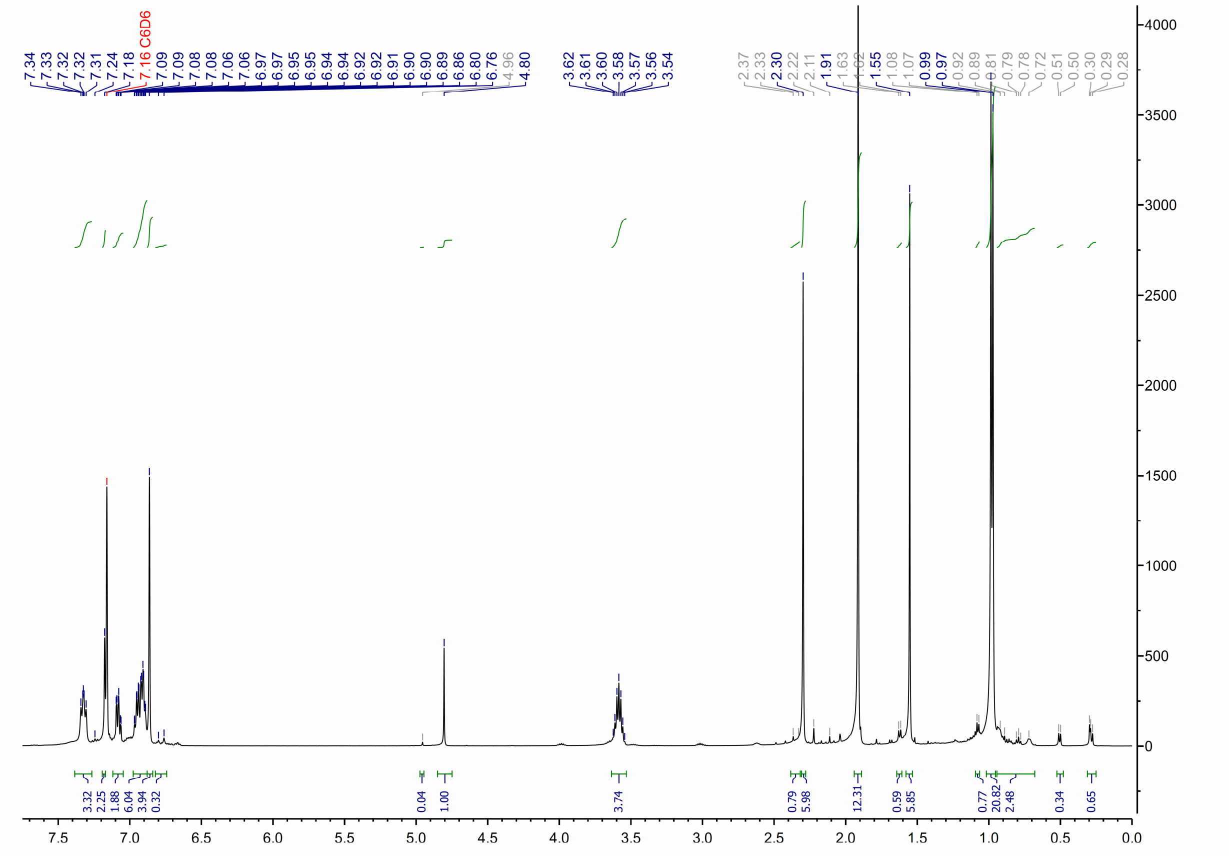

Figure S23. ^{1}H NMR spectrum (499.9 MHz, 295 K) of [{(^{Mes}nacnac)Mg}$_2$] **1c** and two equivalents of [{Ph$_2$P(NDip)$_2$}Li] **6** before heating.

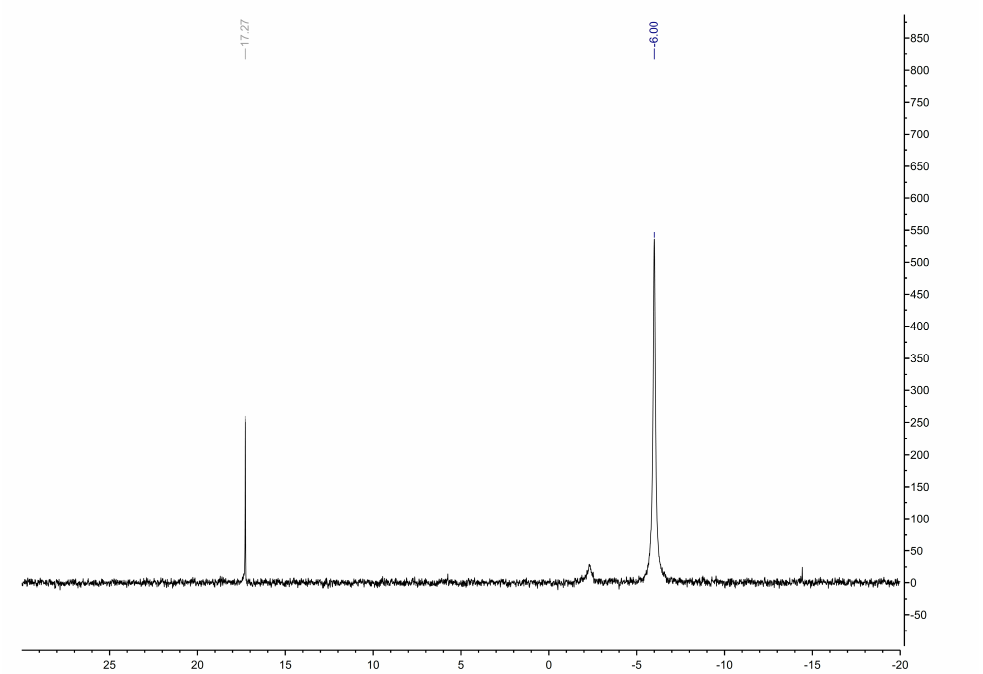

Figure S24. ^{31}P{^{1}H} NMR spectrum (202.4 MHz, 295 K) of [{(^{Mes}nacnac)Mg}$_2$] **1c** and two equivalents of [{Ph$_2$P(NDip)$_2$}Li] **6** before heating.

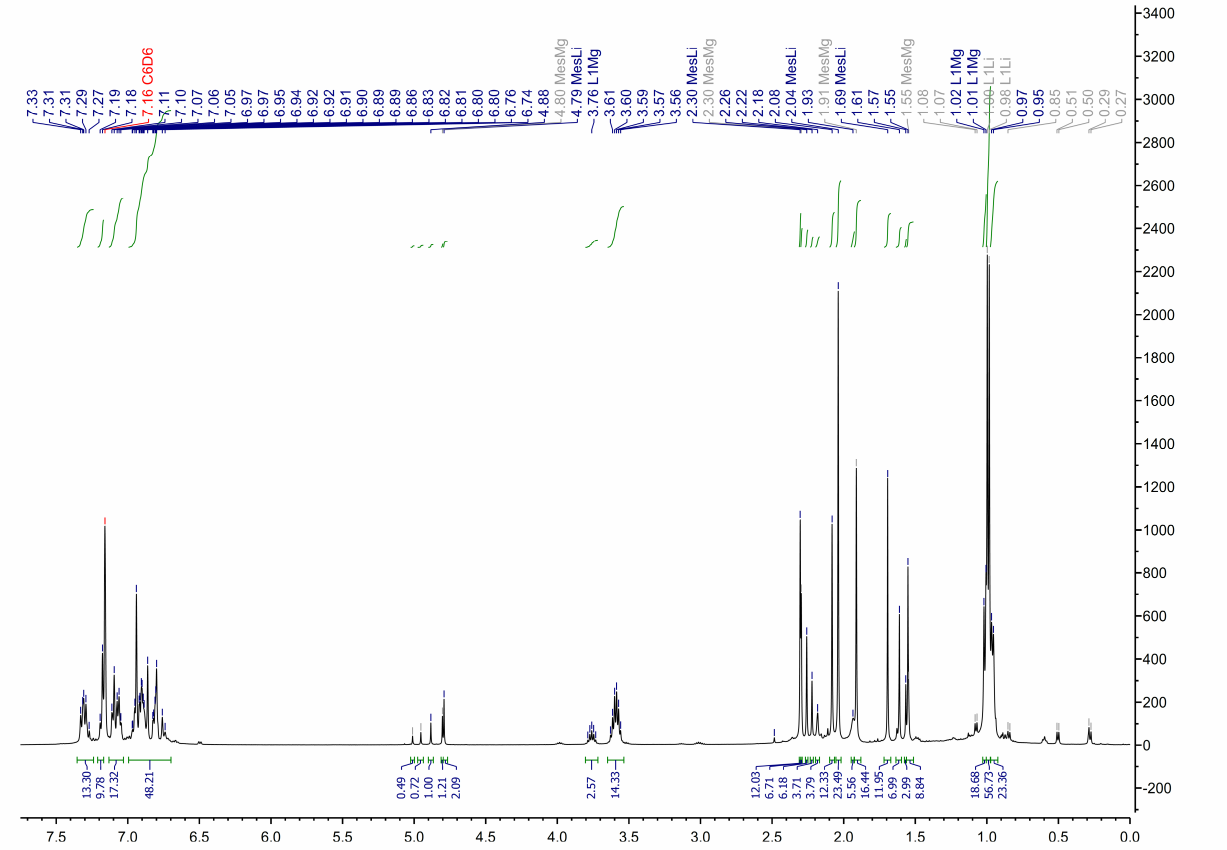

Figure S25. ^{1}H NMR spectrum (499.9 MHz, 295 K) of the reaction between [{($^{\text{Mes}}$nacnac)Mg}$_2$] **1c** and two equivalents of [{Ph$_2$P(NDip)$_2$}Li] **6** after heating at 50°C for 3.5 days.

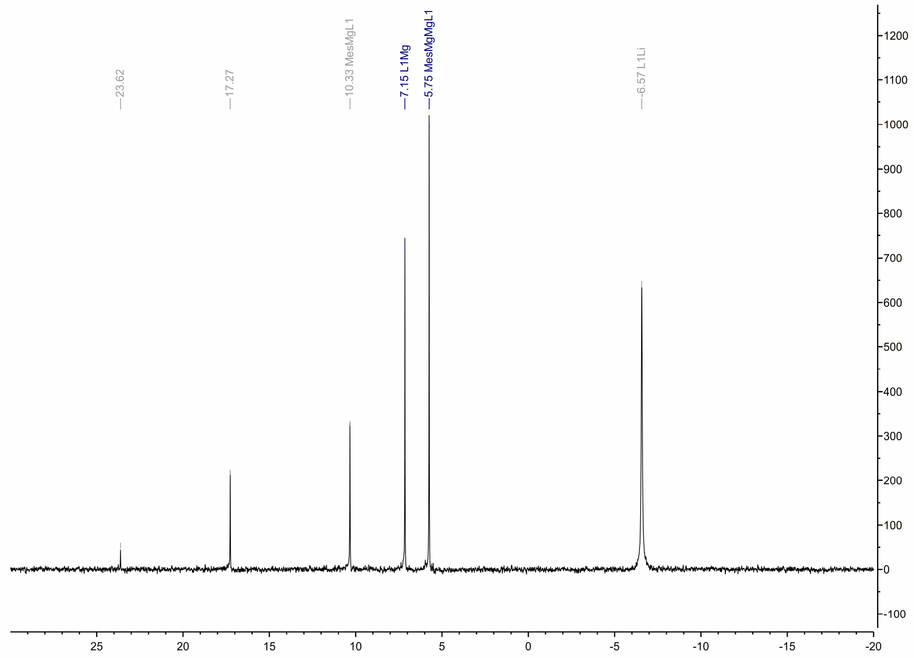

Figure S26. ^{31}P{^{1}H} NMR spectrum (202.4 MHz, 295 K) of the reaction between [{($^{\text{Mes}}$nacnac)Mg}$_2$] **1c** and two equivalents of [{Ph$_2$P(NDip)$_2$}Li] **6** after heating at 50°C for 3.5 days.

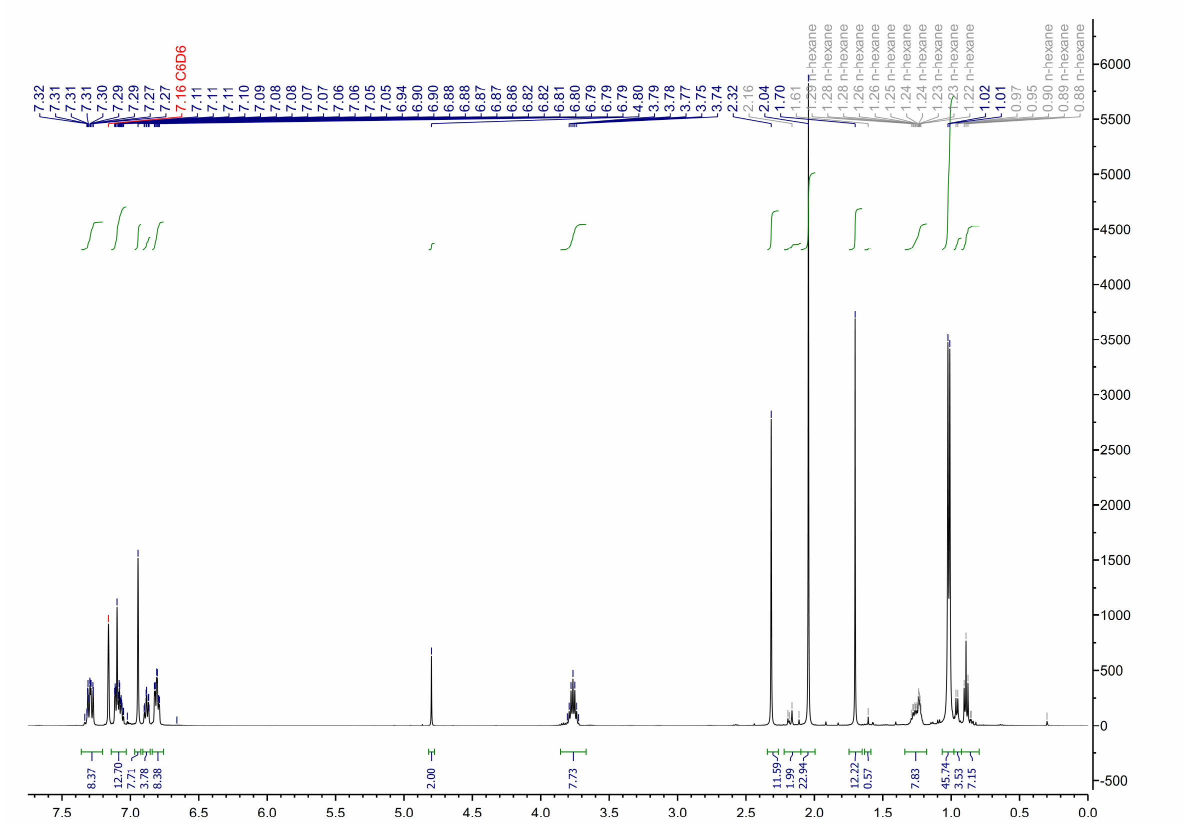

Figure S27. ^{1}H NMR spectrum (499.9 MHz, 295 K) of [({$Ph_2P(NDip)_2$}Mg)$_2$] **2** and two equivalents of [(^{Mes}nacnac)Li] **5c** before heating.

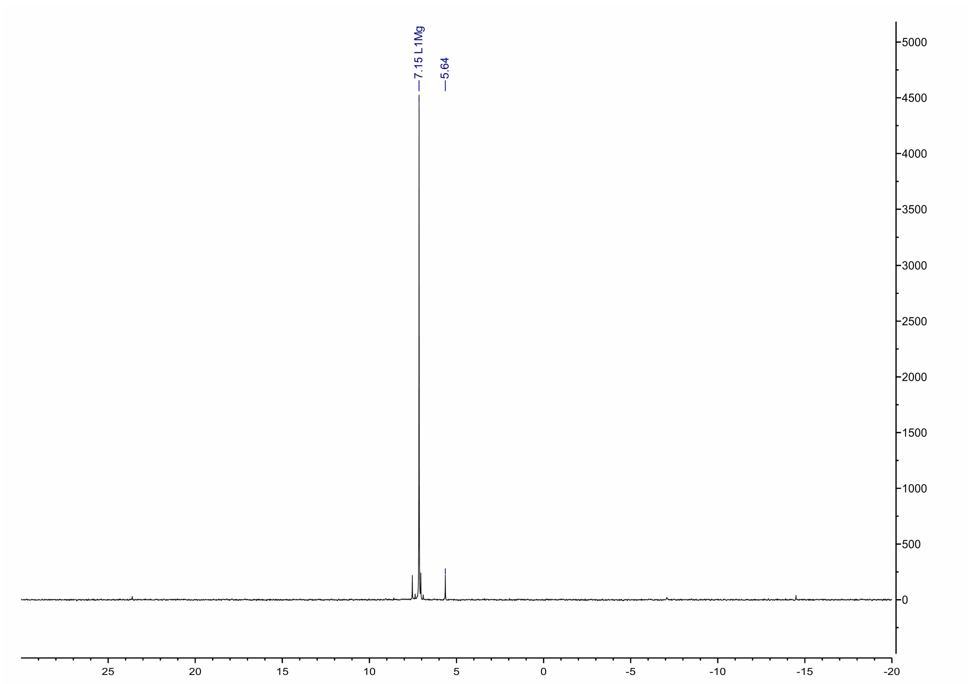

Figure S28. ^{31}P{^{1}H} NMR spectrum (202.4 MHz, 295 K) of [({$Ph_2P(NDip)_2$}Mg)$_2$] **2** and two equivalents of [(^{Mes}nacnac)Li] **5c** before heating.

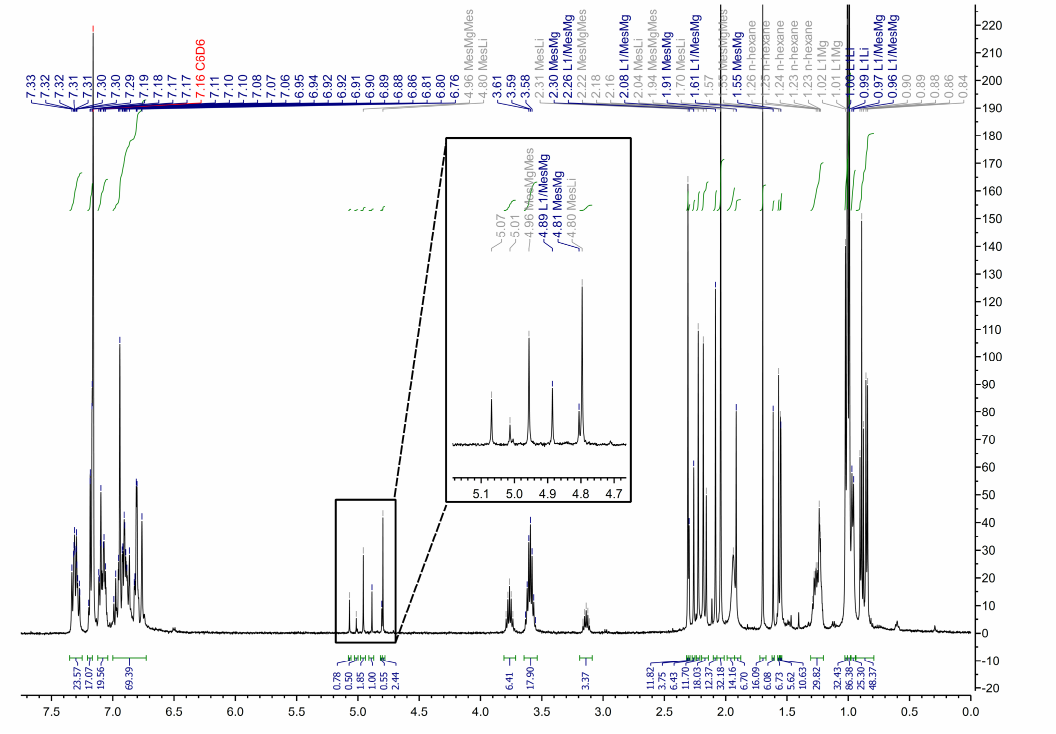

Figure S29. ^{1}H NMR spectrum (499.9 MHz, 295 K) of the resting equilibrium between [({Ph$_2$P(NDip)$_2$}Mg)$_2$] **2** and two equivalents of [(^{Mes}nacnac)Li] **5c** after heating at 50°C for six days.

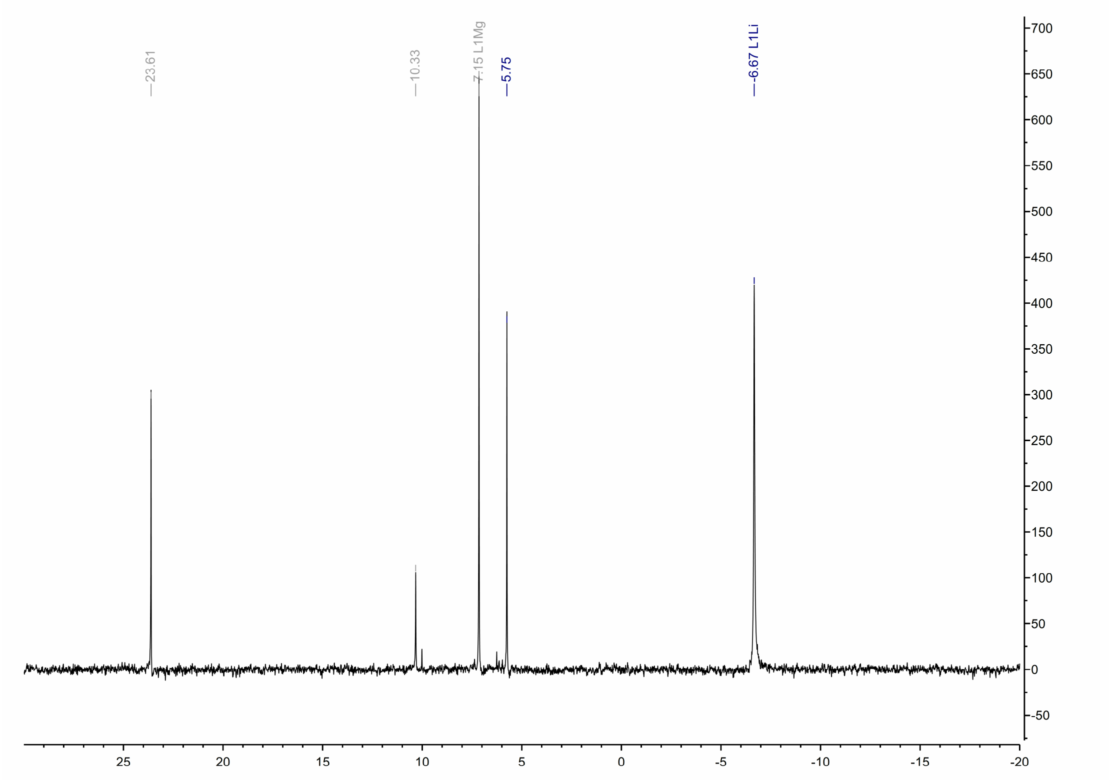

Figure S30. ^{31}P{^{1}H} NMR spectrum (202.4 MHz, 295 K) of the resting equilibrium between [({Ph$_2$P(NDip)$_2$}Mg)$_2$] **2** and two equivalents of [(^{Mes}nacnac)Li] **5c** after heating at 50°C for six days.

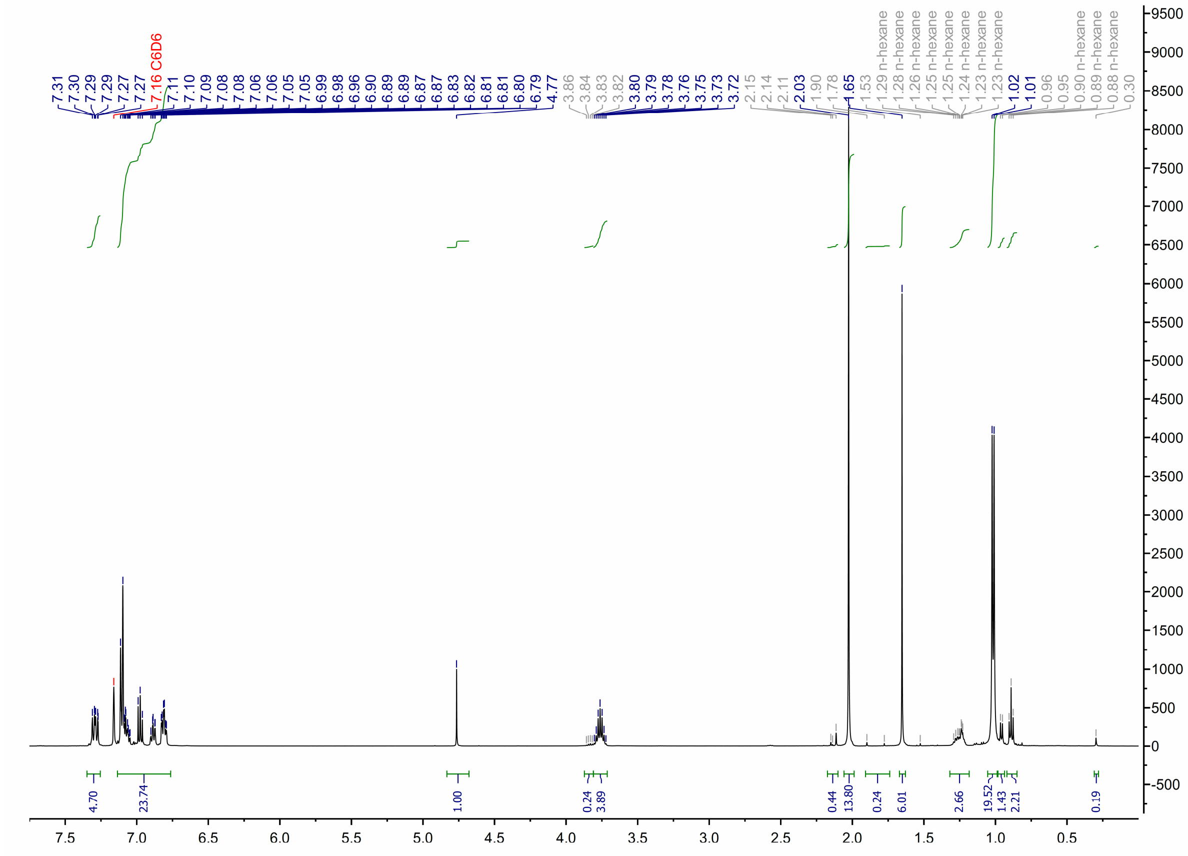

Figure S31. ^{1}H NMR spectrum (499.9 MHz, 298 K) spectrum of [({Ph$_2$P(NDip)$_2$}Mg)$_2$] **2** and [(^{Xyl}nacnac)Li] **5d** before heating.

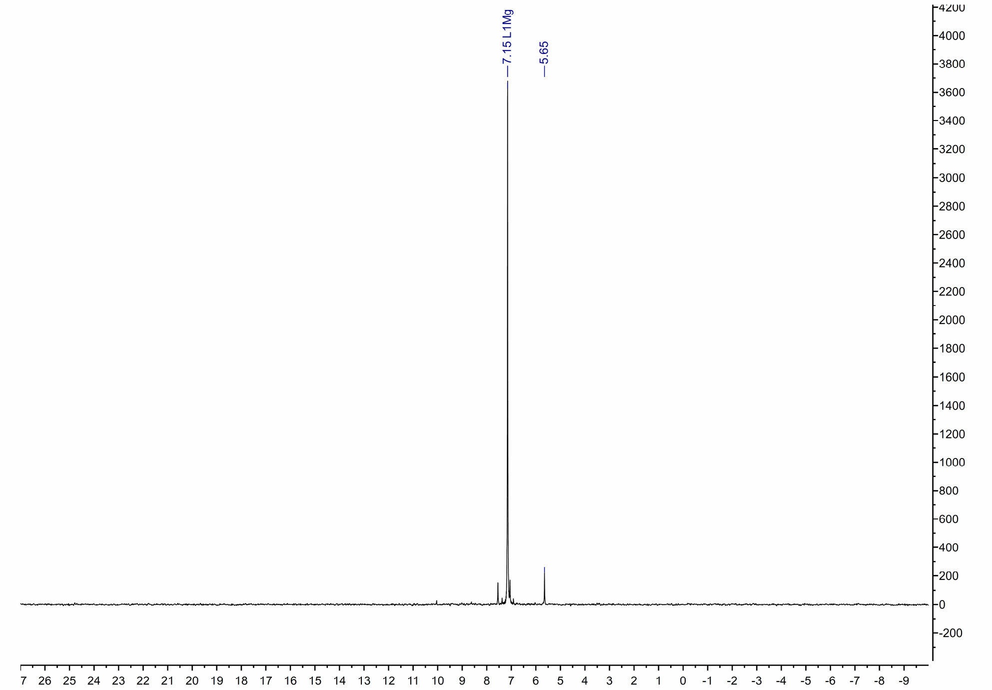

Figure S32. ^{31}P{^{1}H} NMR spectrum (202.4 MHz, 295 K) of [({Ph$_2$P(NDip)$_2$}Mg)$_2$] **2** and two equivalents of [(^{Xyl}nacnac)Li] **5d** before heating.

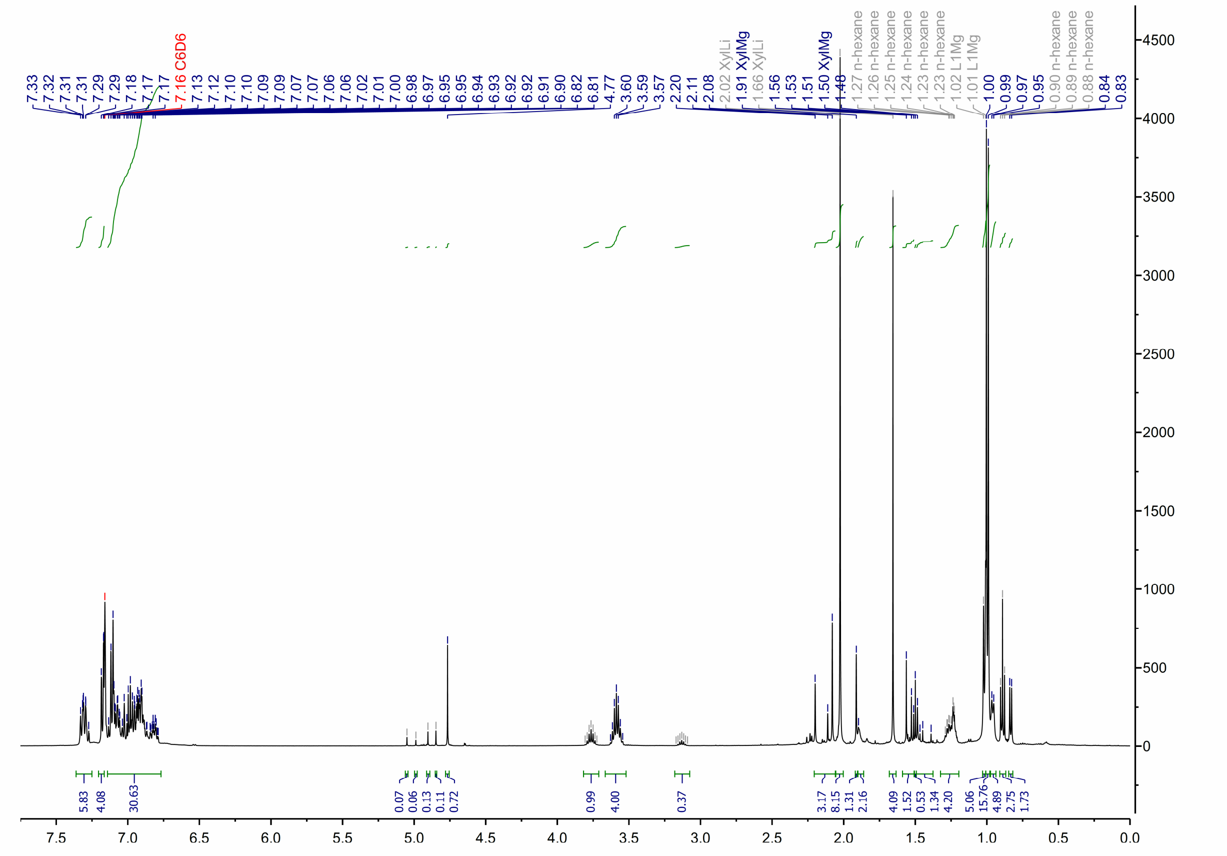

Figure S33. ^{1}H NMR (499.9 MHz, 295 K) spectrum of the reaction mixture of [({$Ph_2P(NDip)_2$}Mg)$_2$] **2** and two equivalents of [(^{Xyl}nacnac)Li] **5d** after heating at 50°C for 39 days.

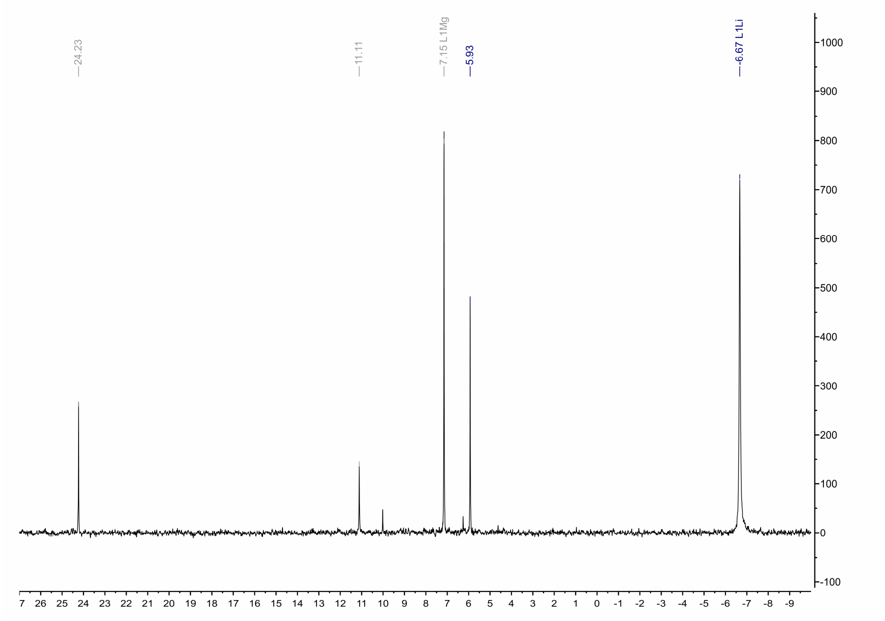

Figure S34. ^{31}P{^{1}H} NMR spectrum (202.4 MHz, 295 K) of the reaction mixture of [({$Ph_2P(NDip)_2$}Mg)$_2$] **2** and two equivalents of [(^{Xyl}nacnac)Li] **5d** after heating at 50°C for 39 days; further details see next pages.

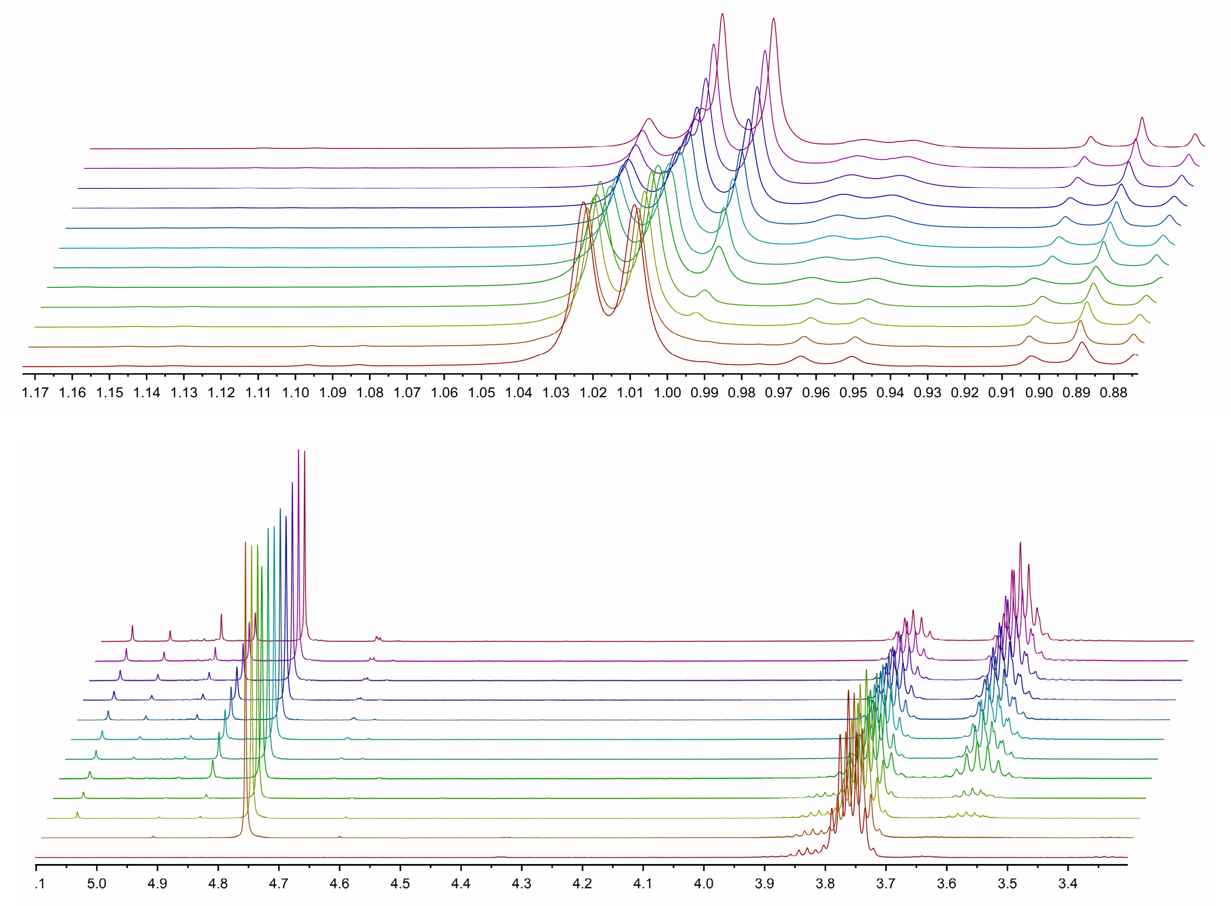

Figure S35. Partial ^{1}H NMR (499.9 MHz, 295 K) time plot spectra, two regions, of the reaction of $[(\{Ph_2P(NDip)_2\}Mg)_2]$ **2** with two equivalents of $[(^{Xyl}nacnac)Li]$ **5d** at 50°C over the course of 39 days. Top: the resonance for **2** (δ = 1.01 ppm (d) of the $Ph_2P(NDip)_2$ $CH(CH_3)_2$ groups) decrease over time whilst those for $[\{Ph_2P(NDip)_2\}MgMg(^{Xyl}nacnac)]$ **7d** (δ = 0.99 ppm (d)) and $[\{Ph_2P(NDip)_2\}Li]$ **6** (δ = 0.99 ppm (d)) increase. Bottom: the backbone γ-C*H* resonances (δ = 4.77 ppm) overlap for $[(^{Xyl}nacnac)Li]$ **5d**, $[\{Ph_2P(NDip)_2\}MgMg(^{Xyl}nacnac)]$ **7d** and $[\{(^{Xyl}nacnac)Mg\}_2]$ **1d**. The resonance for **2** (δ = 3.76 ppm (sept)) decreases over time whilst those for $[\{Ph_2P(NDip)_2\}MgMg(^{Xyl}nacnac)]$ **7d** (δ = 3.59 ppm (sept)) and $[\{Ph_2P(NDip)_2\}Li]$ **6** (δ = 3.59 ppm (sept)) increase.

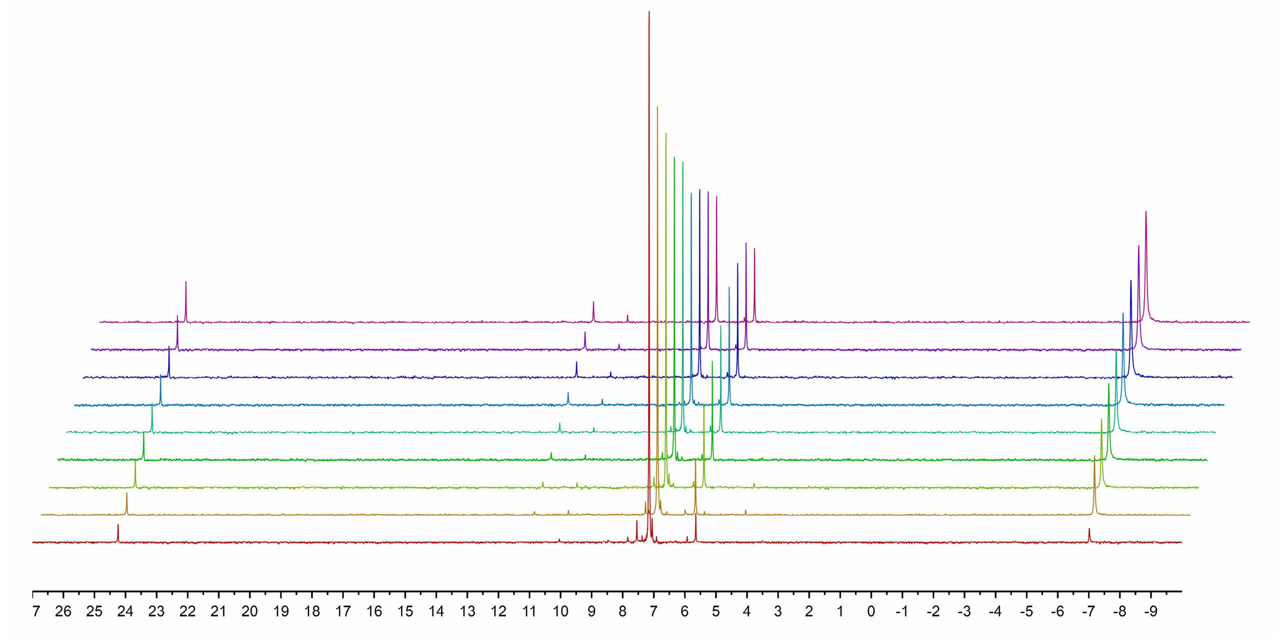

Figure S36. $^{31}P\{^1H\}$ NMR (202.4 MHz, 295 K) time plot spectra of the reaction of $[(\{Ph_2P(NDip)_2\}Mg)_2]$ **2** with two equivalents of $[(^{Xyl}nacnac)Li]$ **5d** at 50°C over the course of 39 days accompanying the ^1H NMR spectra in Figure S33. The resonance for **2** (δ = 7.2 ppm) decreases over time whilst those for $[\{Ph_2P(NDip)_2\}MgMg(^{Xyl}nacnac)]$ **7d** (δ = 5.9 ppm) and $[\{Ph_2P(NDip)_2\}Li]$ **6** (δ = -6.7 ppm) increase.

2.4 Fulleride complex [({$Ph_2P(NDip)_2$}Mg)$_6$C$_{60}$] 8

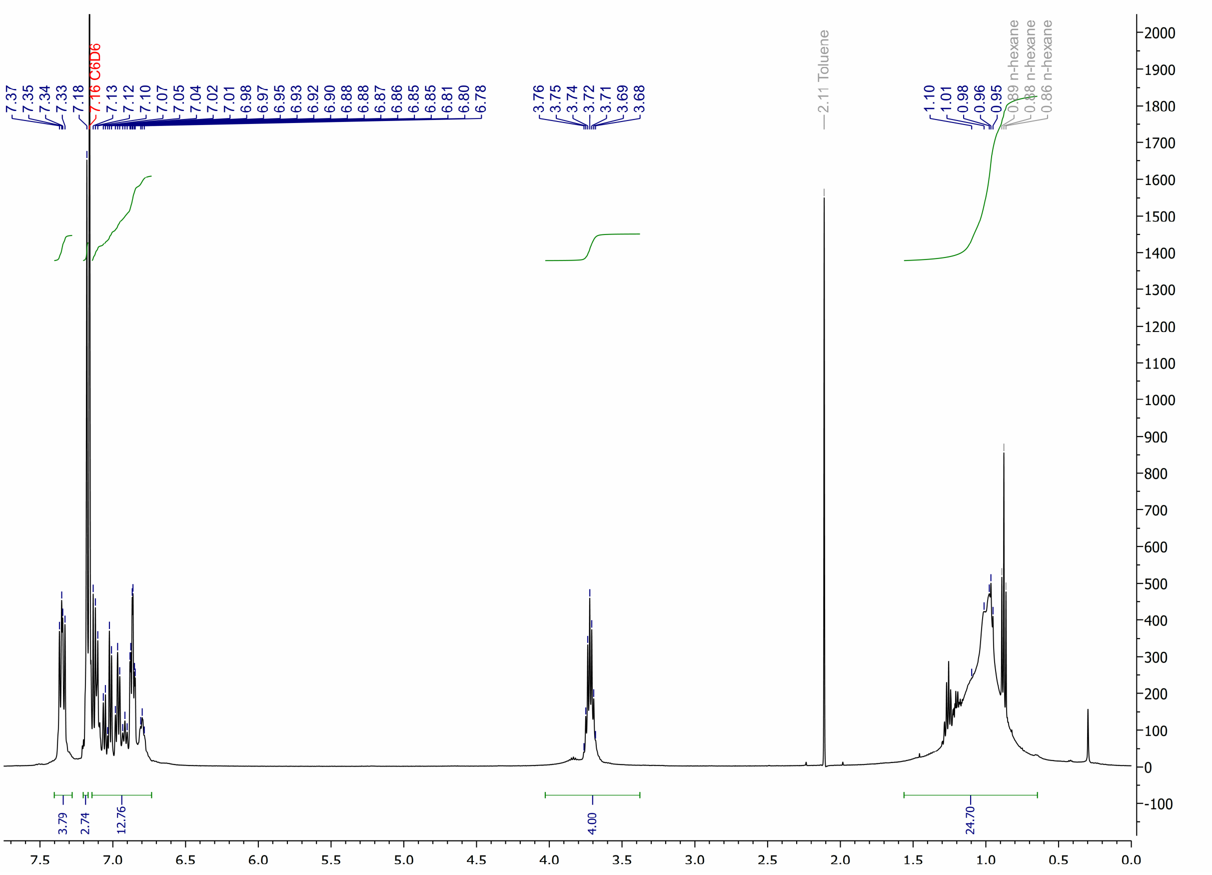

Figure S37. ^{1}H NMR spectrum (499.9 MHz, 293 K) of isolated [({$Ph_2P(NDip)_2$}Mg)$_6$C$_{60}$] **8**.

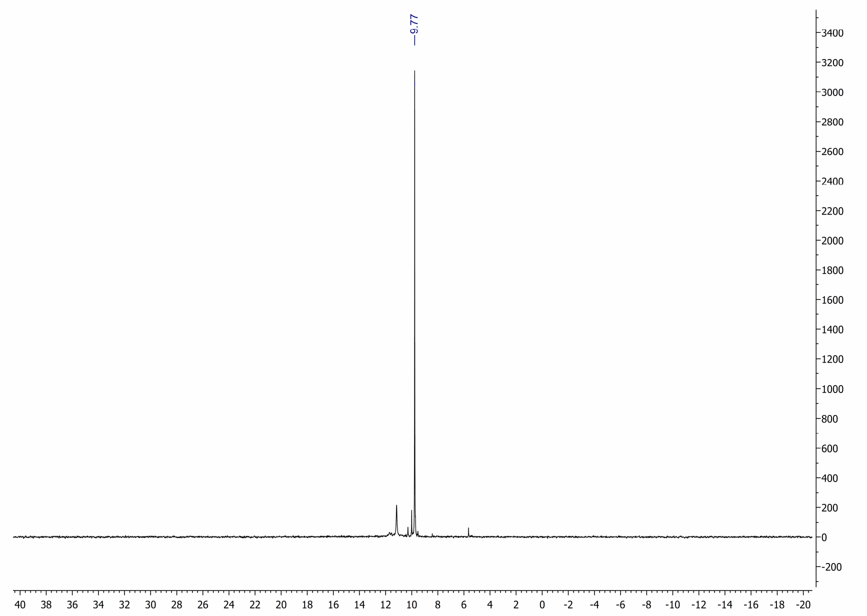

Figure S38. ^{31}P{^{1}H} NMR spectrum (202.4 MHz, 293 K) of isolated [({$Ph_2P(NDip)_2$}Mg)$_6$C$_{60}$] **8**.

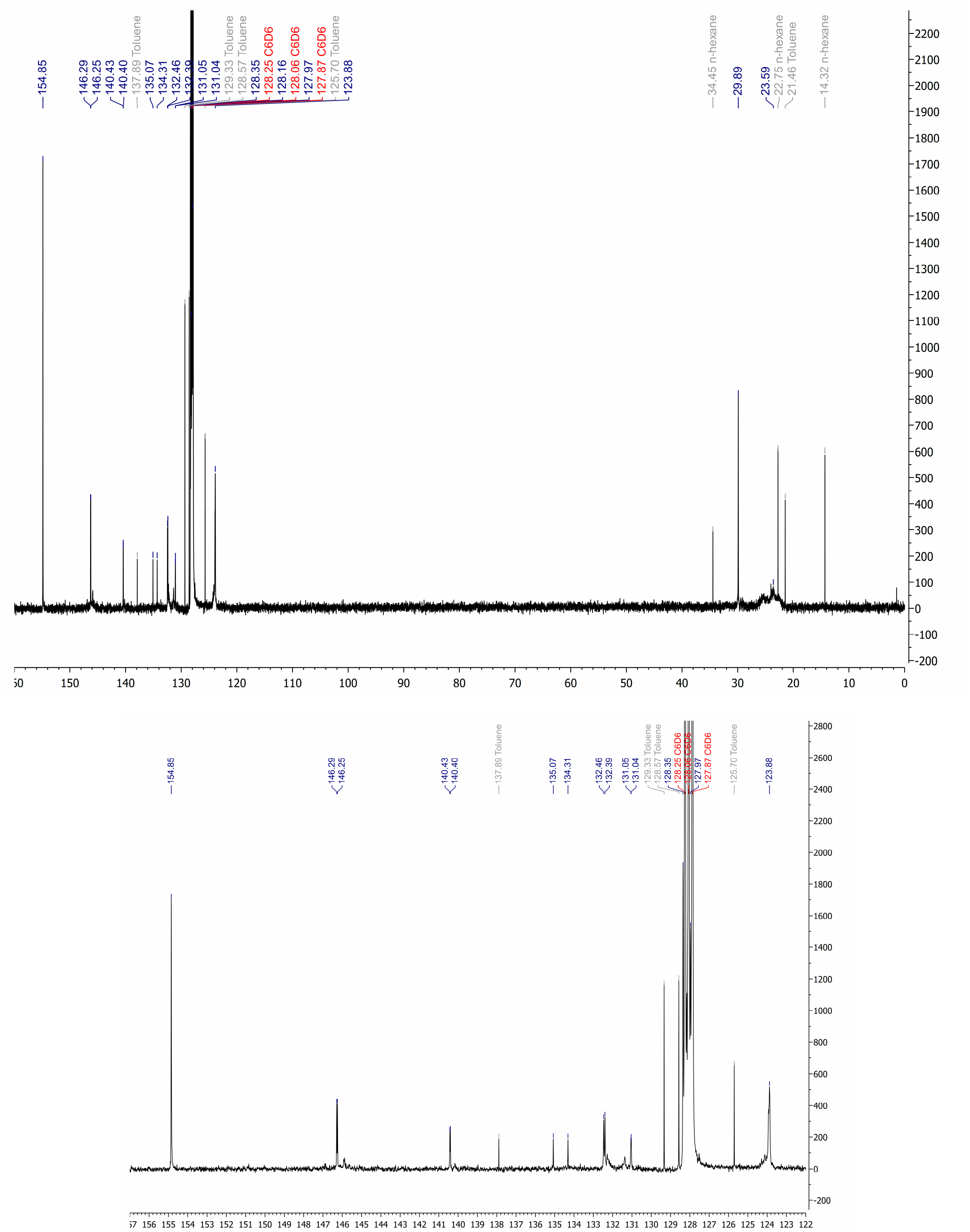

Figure S39. $^{13}C\{^1H\}$ NMR spectrum (125.7 MHz, 293 K) of isolated $[(\{Ph_2P(NDip)_2\}Mg)_6C_{60}]$ **8**.

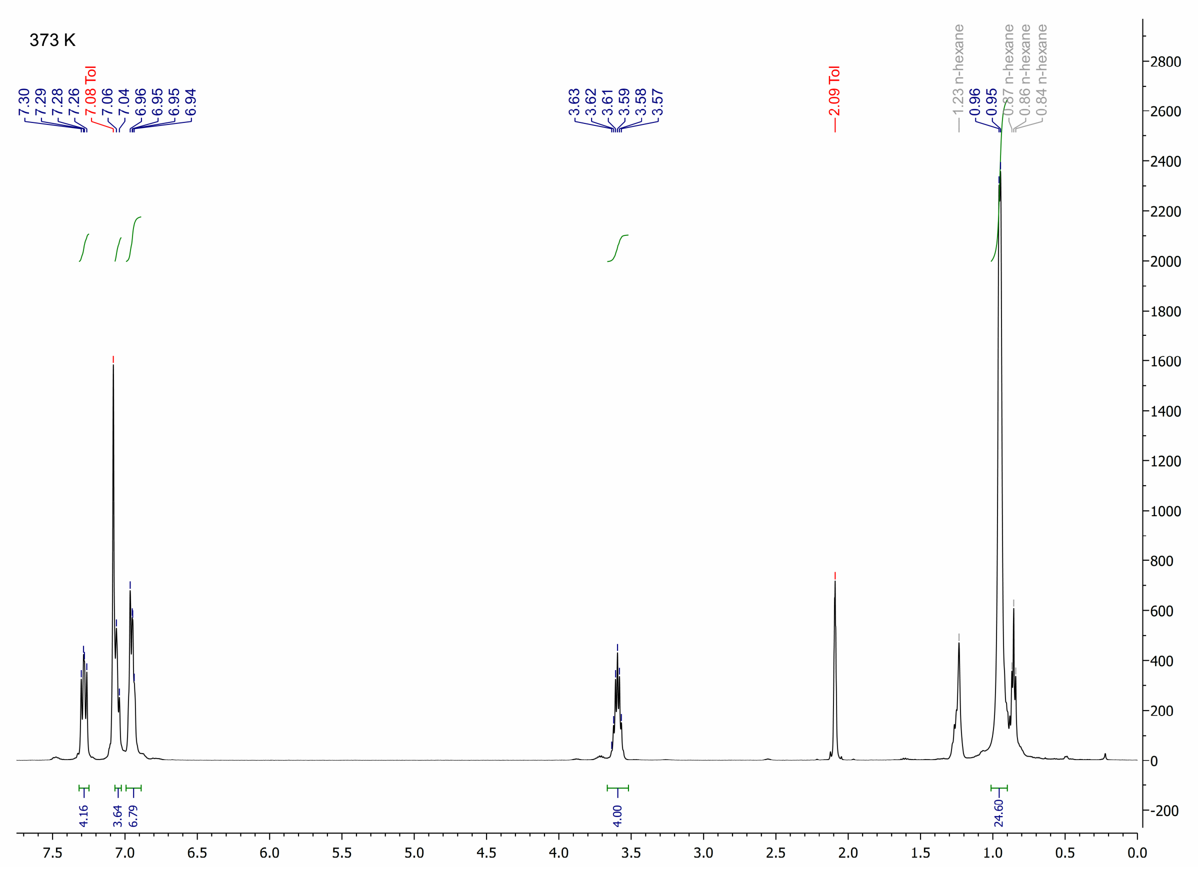

Figure S40. High temperature ^{1}H NMR spectrum (499.9 MHz, 373 K) of isolated [({$Ph_2P(NDip)_2$}Mg)$_6$C$_{60}$] **8** in toluene-d_8.

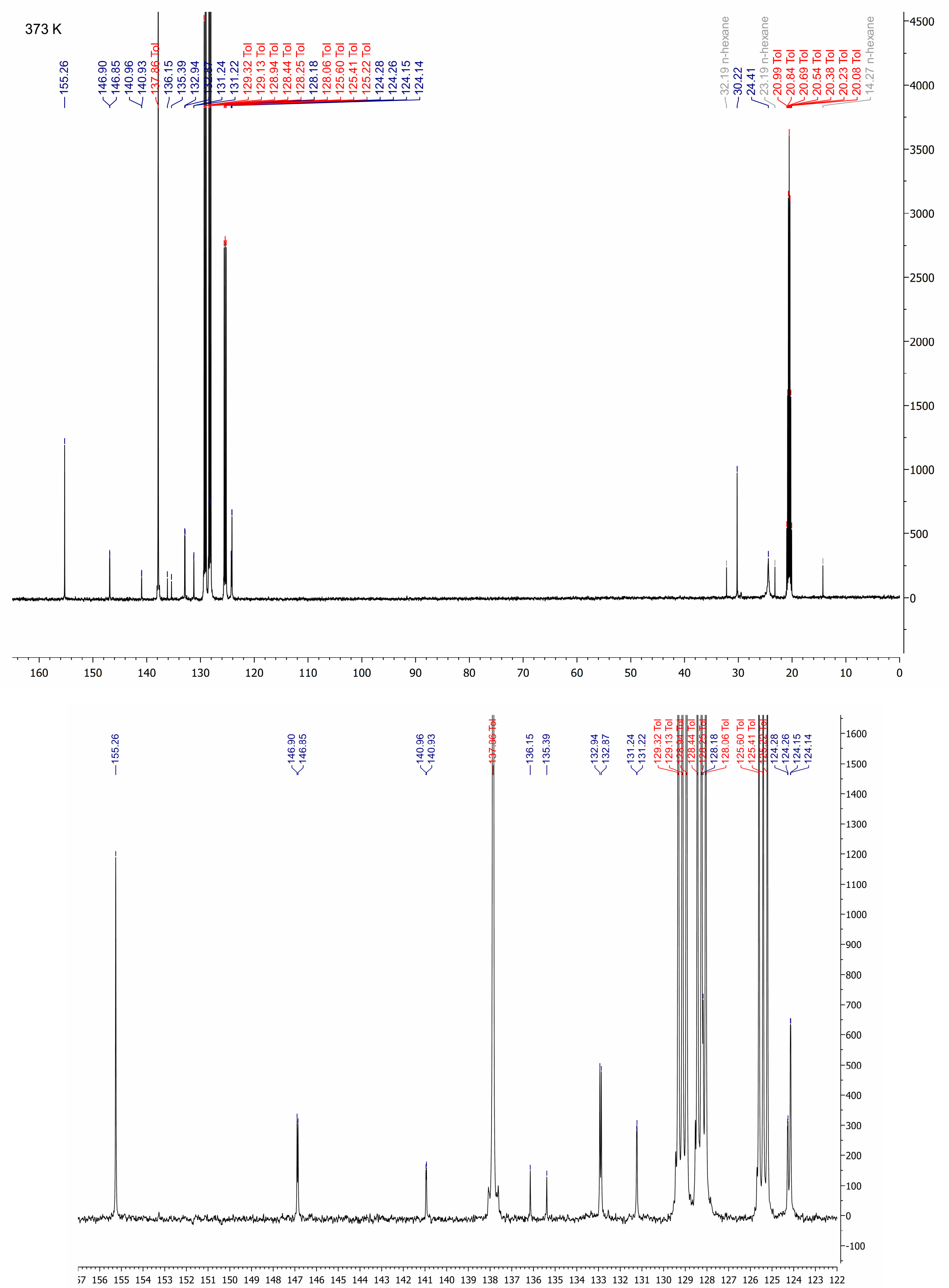

Figure S41. High temperature $^{13}C\{^1H\}$ NMR spectrum (125.7 MHz, 373 K) of isolated $[(\{Ph_2P(NDip)_2\}Mg)_6C_{60}]$ **8** in toluene-d_8 , plus 122-157 ppm region.

3 X-ray crystallography

Suitable crystals of **8'** were mounted in silicone oil and were measured using a Rigaku MM-007HF High Brilliance RA generator/confocal optics with XtaLAB P100 (Cu Kα radiation). Data was collected using CrystalClear.[11] Data were processed (including correction for Lorentz, polarization and absorption) using CrysAlisPro.[12] The structures was solved by dual-space (SHELXT-2018/2)[13] methods and refined by full-matrix least-squares against F^2 using SHELXL-2018/3.[14] Non-hydrogen atoms were refined anisotropically except for the disordered C_{60} unit. Hydrogen atoms were placed in calculated positions (riding model). Severely disordered solvent of crystallisation (hydrocarbons) was removed using the SQUEEZE routine.[15] The removed solvent electron-density is not included in the formula, density, $F(000)$ etc. A description of the individual SQUEEZE details including the volume, number of electrons removed and some residual electron density peaks etc are included in the CIF-file. All calculations were performed using either the CrystalStructure[16] or Olex2[17] interface, except for SQUEEZE, which was accessed via PLATON.[18] Detail on the structure determination and refinement are given below, and in the CIF-file. CCDC 1914904 contains the supplementary crystallographic data for this paper. These data can be obtained free of charge via https://www.ccdc.cam.ac.uk/structures/.

Compound 8'

Crystallographic data: Chemical formula: $C_{276}H_{264}Mg_6N_{12}P_6$, Formula weight: 4080.87, Temperature/K: 173(2), Wavelength/Å: 1.54184, Crystal system: Trigonal, Space group: *R*-3, Cell dimensions: a/Å: 21.4770(2), b/Å; 21.4770(2), c/Å: 45.3378(5), Unit cell volume/$Å^3$: 18110.8(4), No. of formula units per unit cell, Z: 3, Density (calc)/ Mg/m^3: 1.122, Absorption coefficient, μ/mm^{-1}: 0.995, $F(000)$: 6498, Theta range/°: 2.568 to 68.294, Reflections collected: 64511, Independent reflections: 7370, R_{int}: 0.0467, Completeness (to theta)/%: 99.9 (67.684°), Data / restraints / parameter: 7370 / 447 / 502, Goodness of fit on F^2: 1.060, Final R_1 value (I > 2σ(I)): 0.0544, Final $wR(F^2)$ value ($I > 2\sigma(I)$): 0.1509, Final R_1 value (all data): 0.0627, Final $wR(F^2)$ value (all data): 0.1582, Largest diff. peak and hole/e·$Å^{-3}$: 0.630 and -0.511, CCDC number: 1914904.

The complex $[(\{Ph_2P(NDip)_2\}Mg)_6C_{60}]\cdot 4C_5H_{12}$, **8'**, see main text, crystallised with one sixth of the molecule in the asymmetric unit. A space-filling model is shown in Figure S40. The independent $[\{Ph_2P(NDip)_2\}Mg]^+$ unit is well ordered though the C_{60} unit is severely disordered. It was modelled by constructing two independent full C_{60} models (with one-sixth-occupancy atoms and with bonds to symmetry-related atoms suppressed), constrained to idealised geometries, in the asymmetric unit and their contributions were freely refined isotropically to 68.7 and 31.3%, respectively, resulting in twelve positions for each carbon atom in C_{60}. The final model was refined with restraints to thermal motion for the C_{60} section. Although no information about Mg···C interactions can be taken from this structure, an overall approximate octahedral arrangement of the $[\{Ph_2P(NDip)_2\}Mg]^+$ heterocycles around the C_{60} unit is observed. Thus it is likely that Mg···C interactions involving five-membered rings, six-membered rings and C-C bonds are present due to symmetry. Solvent of crystallisation, *n*-pentane, was removed using the SQUEEZE routine (Solvent Accessible Volume per unit cell = 2663 Å^3, # Electrons Found in S.A.V. = 488).

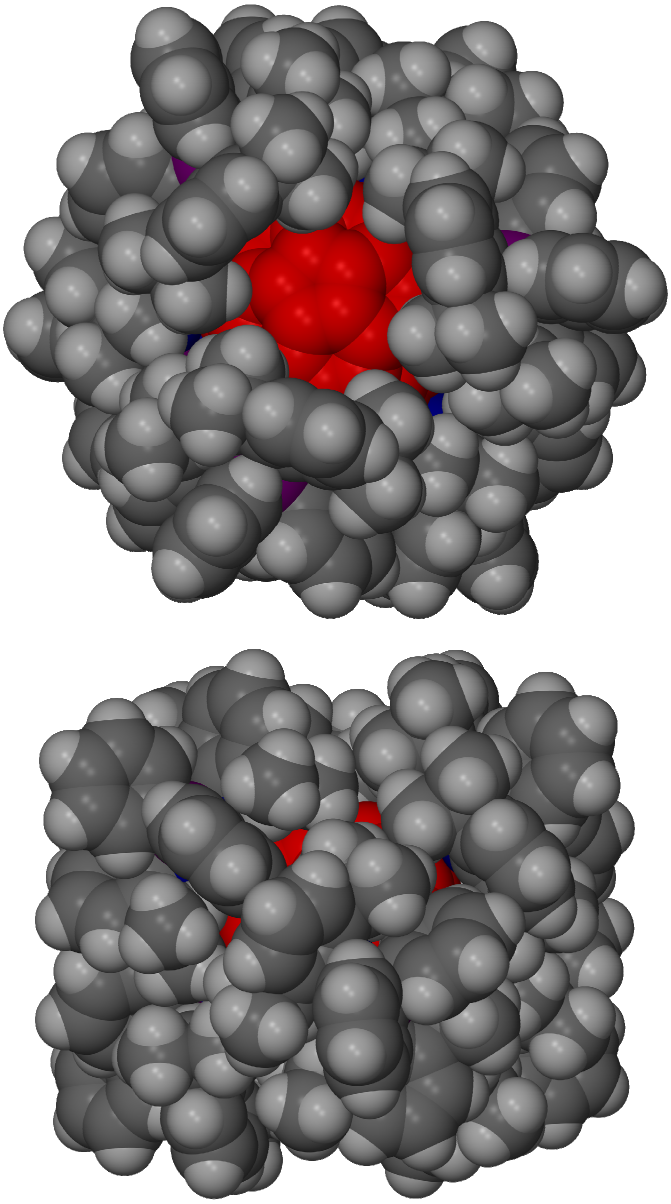

Figure S42. Space-filling model (two views) for **8'** (C_{60} red, P violet, Mg green, N blue, C grey).

4 References

1 S. P. Green, C. Jones and A. Stasch, *Science*, 2007, **318**, 1754–1757.

2 R. Lalrempuia, C. E. Kefalidis, S. J. Bonyhady, B. Schwarze, L. Maron, A. Stasch and C. Jones, *J. Am. Chem. Soc.*, 2015, **137**, 8944–8947.

3 S. J. Bonyhady, C. Jones, S. Nembenna, A. Stasch, A. J. Edwards and G. J. McIntyre, *Chem. Eur. J.*, 2010, **16**, 938–955.

4 (a) S. J. Bonyhady, D. Collis, N. Holzmann, A. J. Edwards, R. O. Piltz, G, Frenking, A. Stasch and C. Jones, *Nat. Commun.*, 2018, **9**, 3079; (b) A. Stasch and C. Jones, *Dalton Trans.*, 2011, **40**, 5659–5672.

5 (a) J. Hicks, M. Juckel, A. Paparo, D. Dange and C. Jones, *Organometallics,* 2018, **37**, 4810−4813; (b) C. Jones, A. Stasch and A. Boutland, *Inorg. Synth.*, 2018, **37**, 40−45.

6 A. Stasch, *Angew. Chem. Int. Ed.*, 2014, **53**, 10200–10203.

7 A. L. Hawley and A. Stasch, *Eur. J. Inorg. Chem.*, 2015, 258–270.

8 S. R. Lawrence, C. An. Ohlin, D. B. Cordes, A. M. Z. Slawin and A. Stasch, *Chem. Sci.*, 2019, DOI: 10.1039/C9SC03857D.

9 C. Bakewell, A. J. P. White and M. R. Crimmin, *J. Am. Chem. Soc.*, 2016, **138**, 12763–12766.

10 S. Gondzik, C. Wölper, R. Haack, G. Jansen and S. Schultz, *Dalton Trans.*, 2015, **44**, 15703−15711.

11 *CrystalClear-SM Exper*t v2.1. Rigaku Americas, The Woodlands, Texas, USA, and Rigaku Corporation, Tokyo, Japan, 2015.

12 *CrysAlisPro* v1.171.38.46. Rigaku Oxford Diffraction, Rigaku Corporation, Oxford, U.K. 2015.

13 G. M. Sheldrick, *Acta Cryst.*, 2015, **A71**, 3–8.

14 G. M. Sheldrick, *Acta Cryst.*, 2015, **C71**, 3–8.

15 A. L. Spek, *Acta Cryst.*, 2015, **C71**, 9–18.

16 *CrystalStructure* v4.3.0. Rigaku Americas, The Woodlands, Texas, USA, and Rigaku Corporation, Tokyo, Japan, 2018.

17 O. V. Dolomanov, L. J. Bourhis, R. J. Gildea, J. A. K. Howard and H. Puschmann, *J. Appl. Cryst.*, 2009, **42**, 339–341.

18 A. L. Spek, *Acta Crystallogr. Sect D.*, 2009, **65**, 148–155.